

# **The Smaller (SALI) and the Generalized (GALI) Alignment Index methods of chaos detection**

**Haris Skokos**

**Department of Mathematics and Applied Mathematics  
University of Cape Town  
Cape Town, South Africa**

**E-mail: [haris.skokos@uct.ac.za](mailto:haris.skokos@uct.ac.za)**

**URL: [http://math\\_research.uct.ac.za/~hskokos/](http://math_research.uct.ac.za/~hskokos/)**

**Online workshop "Chaos Indicators, Phase Space and Chemical Reaction Dynamics", Bristol, 4-6 May 2020**

# Outline

- **Dynamical Systems**
  - ✓ **Hamiltonian models – Variational equations**
  - ✓ **Symplectic maps – Tangent map**
- **Chaos Indicators**
  - ✓ **Maximum Lyapunov Exponent**
  - ✓ **Smaller ALignment Index – SALI**
    - **Definition**
    - **Behavior for chaotic and regular motion**
    - **Applications**
  - ✓ **Generalized ALignment Index – GALI**
    - **Definition - Relation to SALI**
    - **Behavior for chaotic and regular motion**
    - **Application to time-dependent models**

# Autonomous Hamiltonian systems

Consider an **N degree of freedom** autonomous Hamiltonian system having a Hamiltonian function of the form:

$$H(\overbrace{q_1, q_2, \dots, q_N}^{\text{positions}}, \overbrace{p_1, p_2, \dots, p_N}^{\text{momenta}})$$

The time evolution of an orbit (trajectory) with initial condition

$$P(0) = (q_1(0), q_2(0), \dots, q_N(0), p_1(0), p_2(0), \dots, p_N(0))$$

is governed by the **Hamilton's equations of motion**

$$\frac{dp_i}{dt} = - \frac{\partial H}{\partial q_i}, \quad \frac{dq_i}{dt} = \frac{\partial H}{\partial p_i}$$

# Variational Equations

We use the notation  $\mathbf{x} = (q_1, q_2, \dots, q_N, p_1, p_2, \dots, p_N)^T$ . The **deviation vector** from a given orbit is denoted by

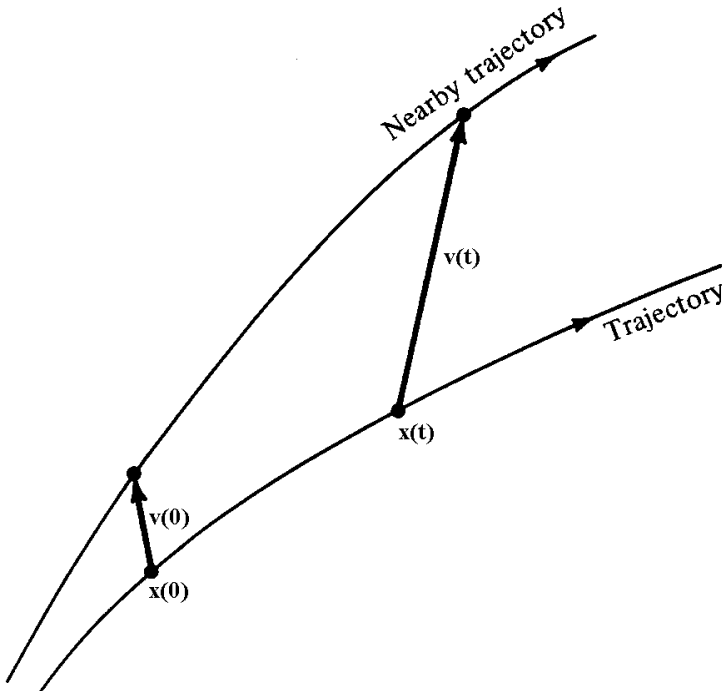
$$\mathbf{v} = (\delta x_1, \delta x_2, \dots, \delta x_n)^T, \text{ with } n=2N$$

The time evolution of  $\mathbf{v}$  is given by the so-called **variational equations**:

$$\frac{d\mathbf{v}}{dt} = -\mathbf{J} \cdot \mathbf{P} \cdot \mathbf{v}$$

where

$$\mathbf{J} = \begin{pmatrix} \mathbf{0}_N & -\mathbf{I}_N \\ \mathbf{I}_N & \mathbf{0}_N \end{pmatrix}, \quad P_{ij} = \frac{\partial^2 H}{\partial x_i \partial x_j} \quad i, j = 1, 2, \dots, n$$



# Symplectic Maps

Consider an **2N-dimensional symplectic map T**. In this case we have **discrete time**.

The evolution of an **orbit** with initial condition

$$P(0)=(x_1(0), x_2(0), \dots, x_{2N}(0))$$

is governed by the **equations of map T**

$$P(i+1)=T P(i) \text{ , } i=0,1,2,\dots$$

The evolution of an initial **deviation vector**

$$v(0) = (\delta x_1(0), \delta x_2(0), \dots, \delta x_{2N}(0))$$

is given by the corresponding **tangent map**

$$v(i+1) = \left. \frac{\partial T}{\partial P} \right|_i \cdot v(i) \text{ , } i = 0, 1, 2, \dots$$

# Maximum Lyapunov Exponent

Roughly speaking, the Lyapunov exponents of a given orbit characterize the **mean exponential rate of divergence** of trajectories surrounding it.

Consider an orbit in the  $2N$ -dimensional phase space with **initial condition**  $\mathbf{x}(0)$  and an **initial deviation vector from it**  $\mathbf{v}(0)$ . Then the mean exponential rate of divergence is:

$$\text{mLCE} = \sigma_1 = \lim_{t \rightarrow \infty} \frac{1}{t} \ln \frac{\|\vec{v}(t)\|}{\|\vec{v}(0)\|}$$

$\sigma_1 = 0 \rightarrow$  Regular motion

$\sigma_1 \neq 0 \rightarrow$  Chaotic motion

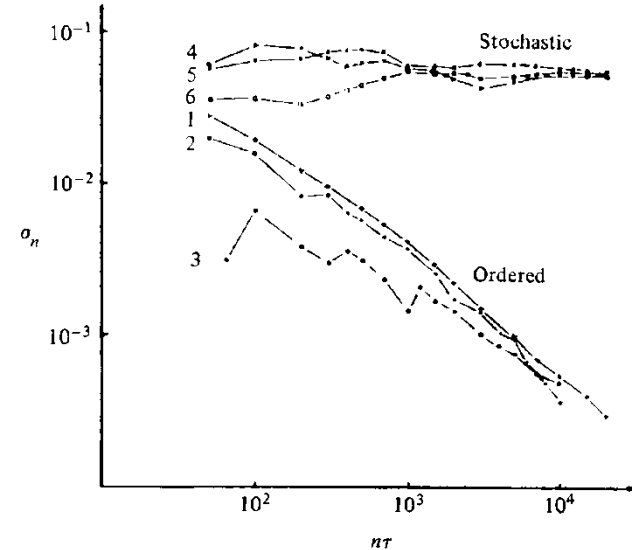


Figure 5.7. Behavior of  $\sigma_n$  at the intermediate energy  $E = 0.125$  for initial points taken in the ordered (curves 1–3) or stochastic (curves 4–6) regions (after Benettin *et al.*, 1976).

If we start with more than one linearly independent deviation vectors they will **align to the direction defined by the largest Lyapunov exponent** for chaotic orbits.

**The  
Smaller ALignment Index  
(SALI)  
method**

# Definition of the SALI

We follow the evolution in time of two different initial deviation vectors ( $\mathbf{v}_1(0)$ ,  $\mathbf{v}_2(0)$ ), and define the SALI (**Ch.S. 2001, J. Phys. A**) as:

$$\text{S A L I}(t) = \min \left\{ \left\| \hat{\mathbf{v}}_1(t) + \hat{\mathbf{v}}_2(t) \right\|, \left\| \hat{\mathbf{v}}_1(t) - \hat{\mathbf{v}}_2(t) \right\| \right\}$$

where

$$\hat{\mathbf{v}}_1(t) = \frac{\mathbf{v}_1(t)}{\|\mathbf{v}_1(t)\|}$$

When the two vectors become **collinear**

$$\text{SALI}(t) \rightarrow 0$$

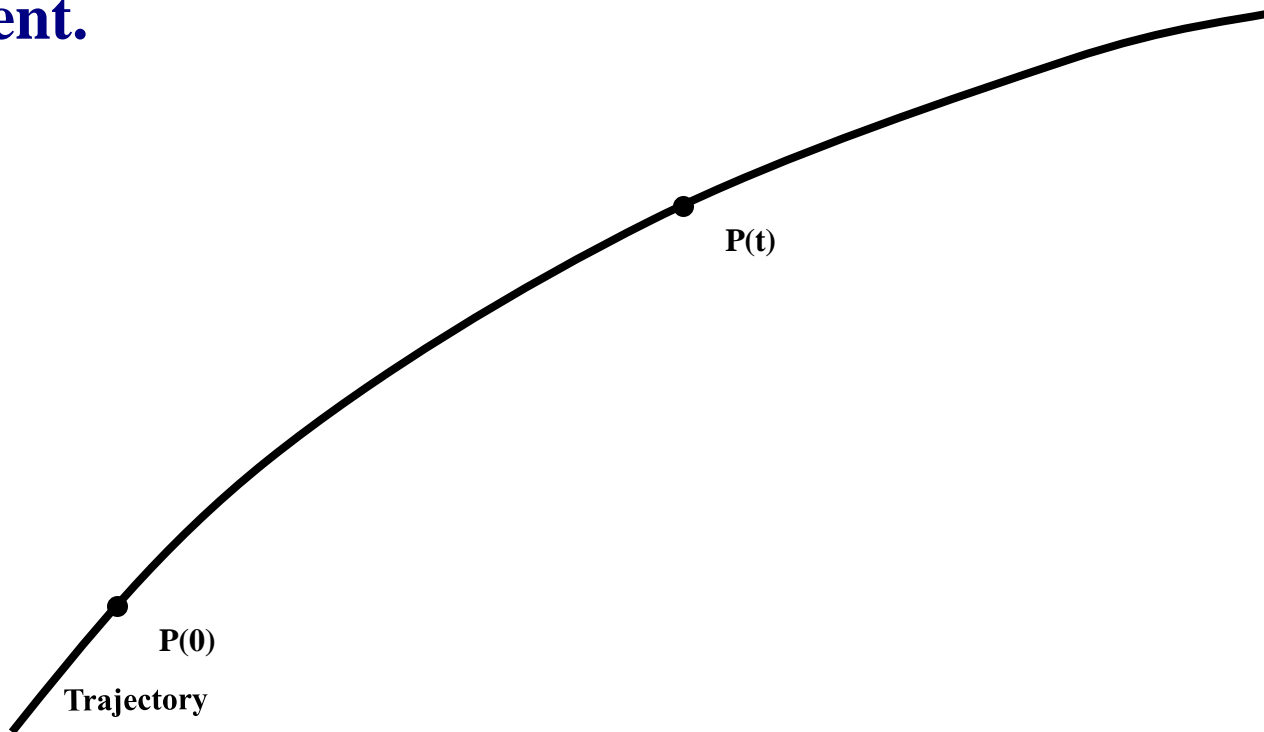


# Behavior of the SALI for chaotic motion

For chaotic orbits the two initially different deviation vectors tend to coincide with the direction defined by the maximum Lyapunov exponent.

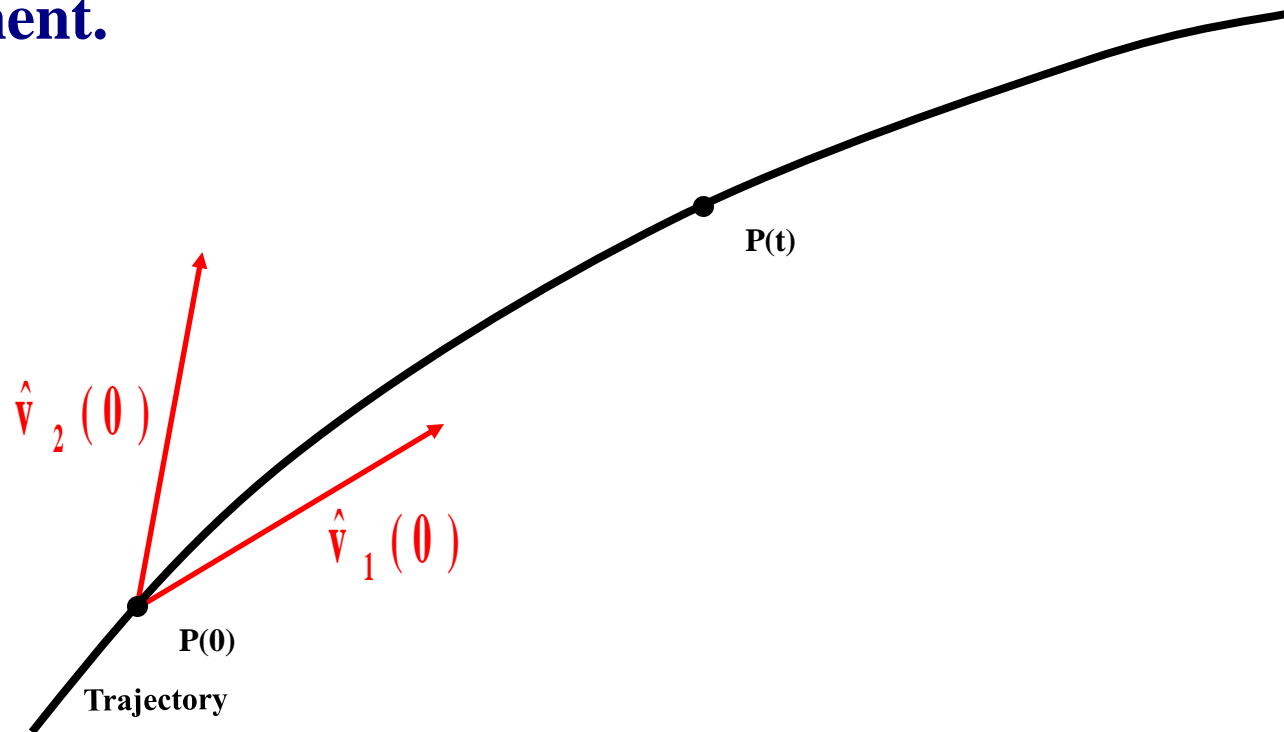
# Behavior of the SALI for chaotic motion

For chaotic orbits the two initially different deviation vectors tend to coincide with the direction defined by the maximum Lyapunov exponent.



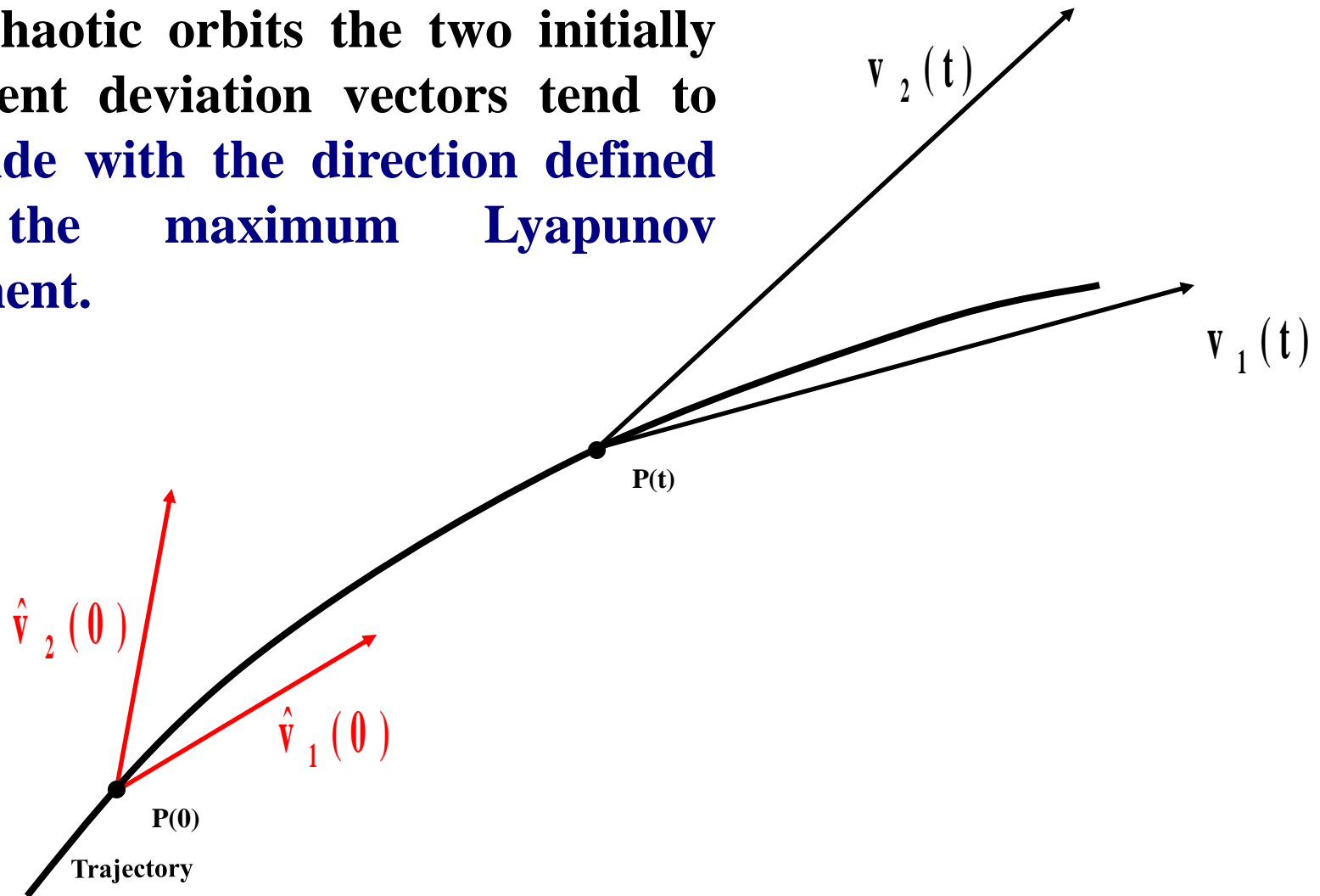
# Behavior of the SALI for chaotic motion

For chaotic orbits the two initially different deviation vectors tend to coincide with the direction defined by the maximum Lyapunov exponent.



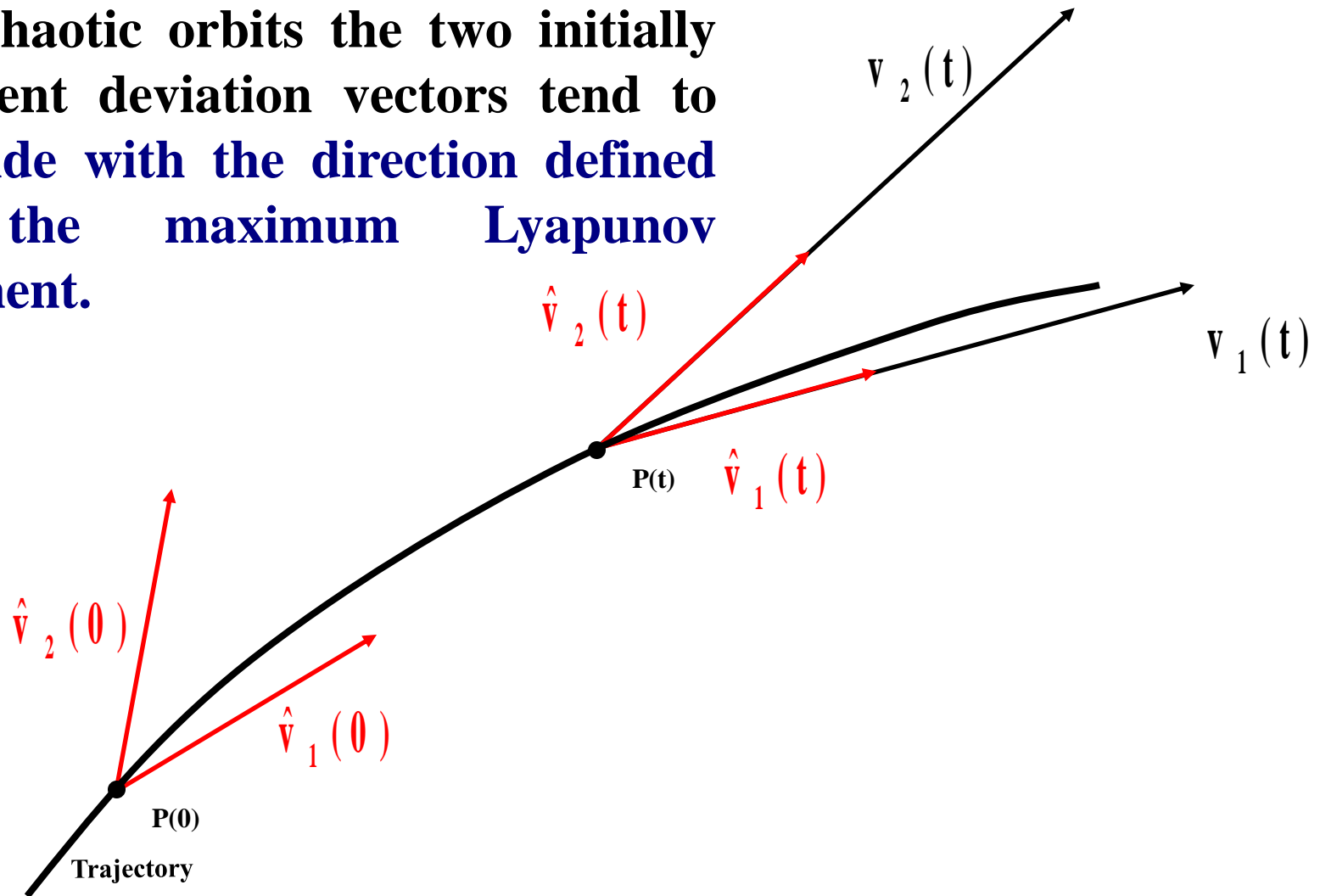
# Behavior of the SALI for chaotic motion

For chaotic orbits the two initially different deviation vectors tend to coincide with the direction defined by the maximum Lyapunov exponent.



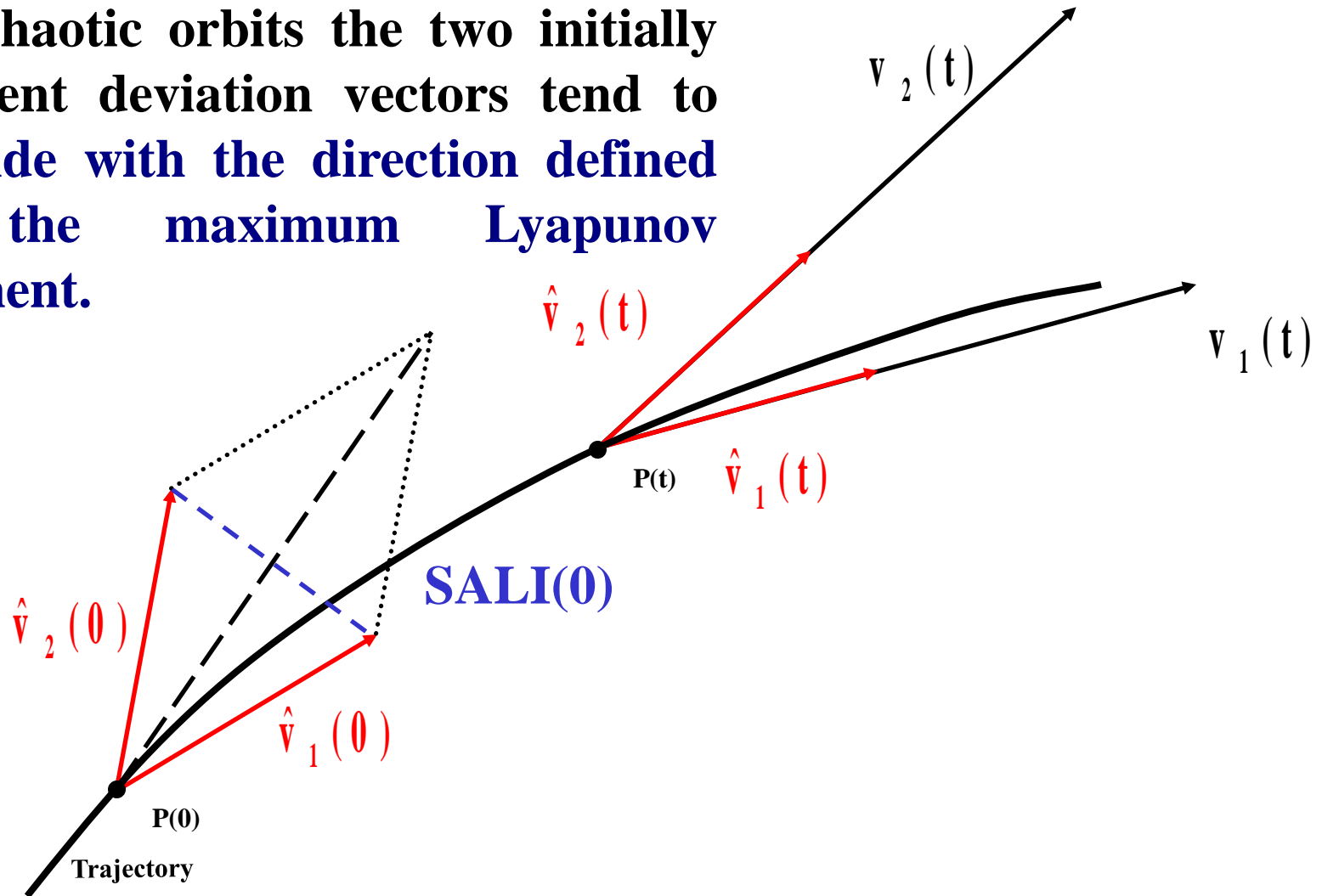
# Behavior of the SALI for chaotic motion

For chaotic orbits the two initially different deviation vectors tend to coincide with the direction defined by the maximum Lyapunov exponent.



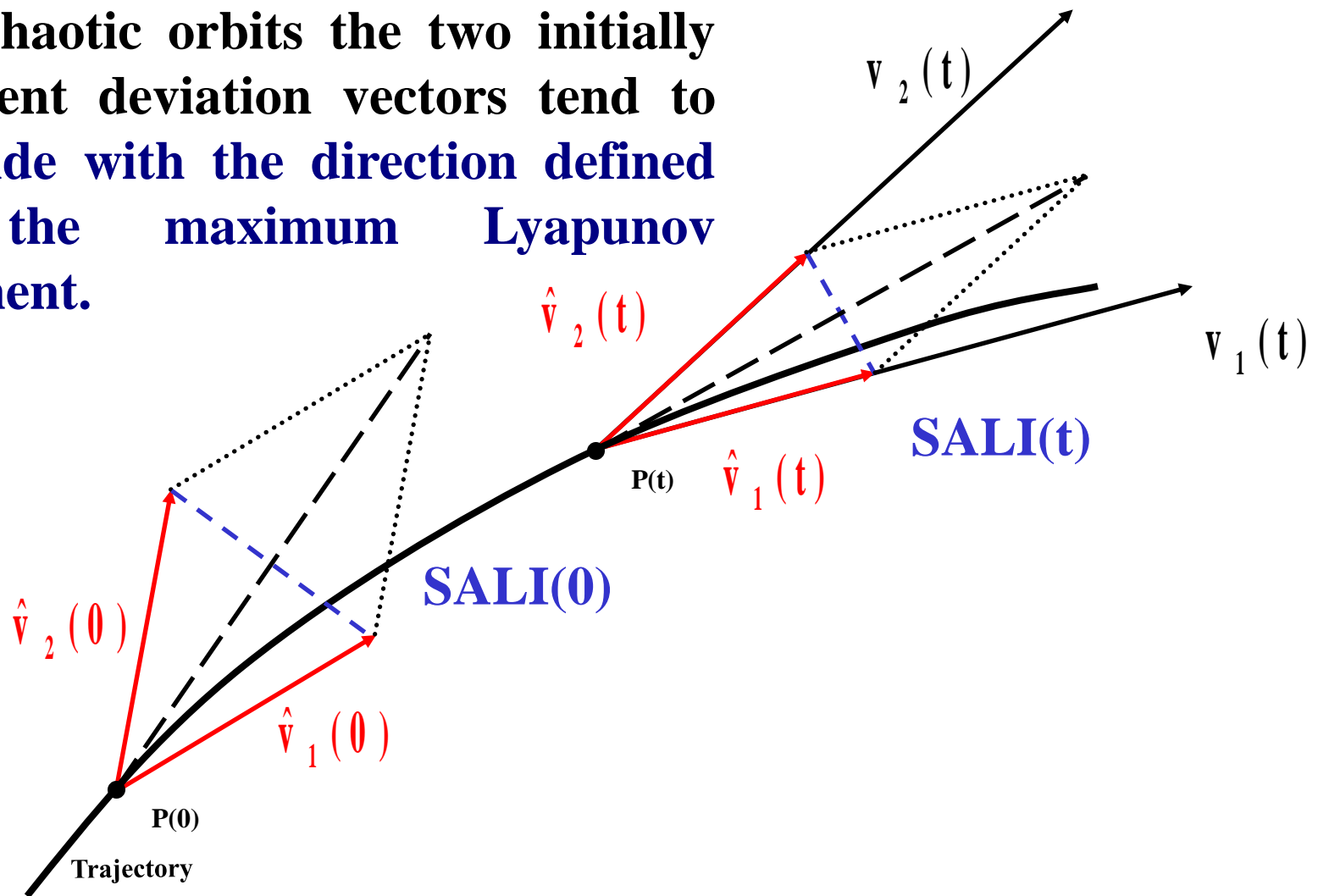
# Behavior of the SALI for chaotic motion

For chaotic orbits the two initially different deviation vectors tend to coincide with the direction defined by the maximum Lyapunov exponent.



# Behavior of the SALI for chaotic motion

For chaotic orbits the two initially different deviation vectors tend to coincide with the direction defined by the maximum Lyapunov exponent.

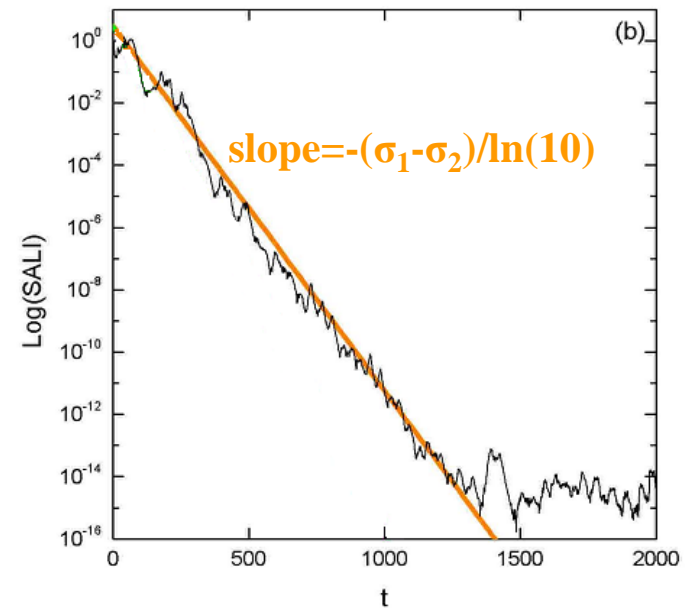
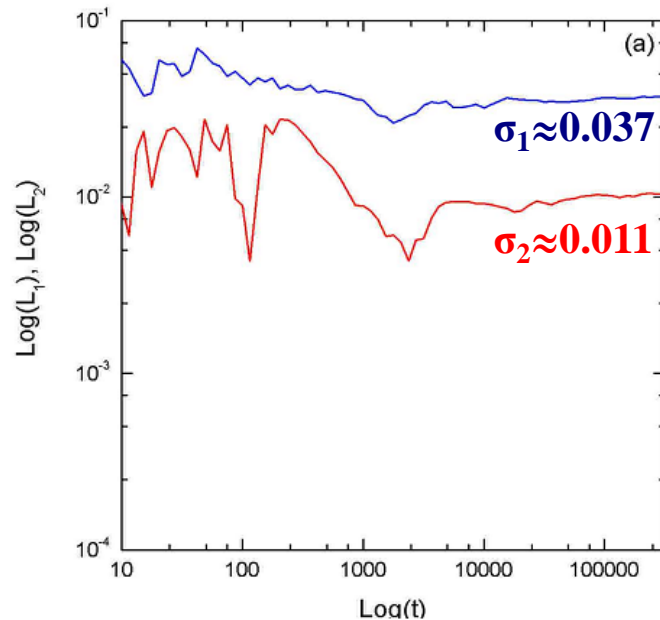


# Behavior of the SALI for chaotic motion

We test the validity of the approximation  $\text{SALI} \propto e^{-(\sigma_1 - \sigma_2)t}$  (Ch.S., Antonopoulos, Bountis, Vrahatis, 2004, J. Phys. A) for a chaotic orbit of the 3D Hamiltonian

$$H = \sum_{i=1}^3 \frac{\omega_i}{2} (q_i^2 + p_i^2) + q_1^2 q_2 + q_1^2 q_3$$

with  $\omega_1=1$ ,  $\omega_2=1.4142$ ,  $\omega_3=1.7321$ ,  $H=0.09$



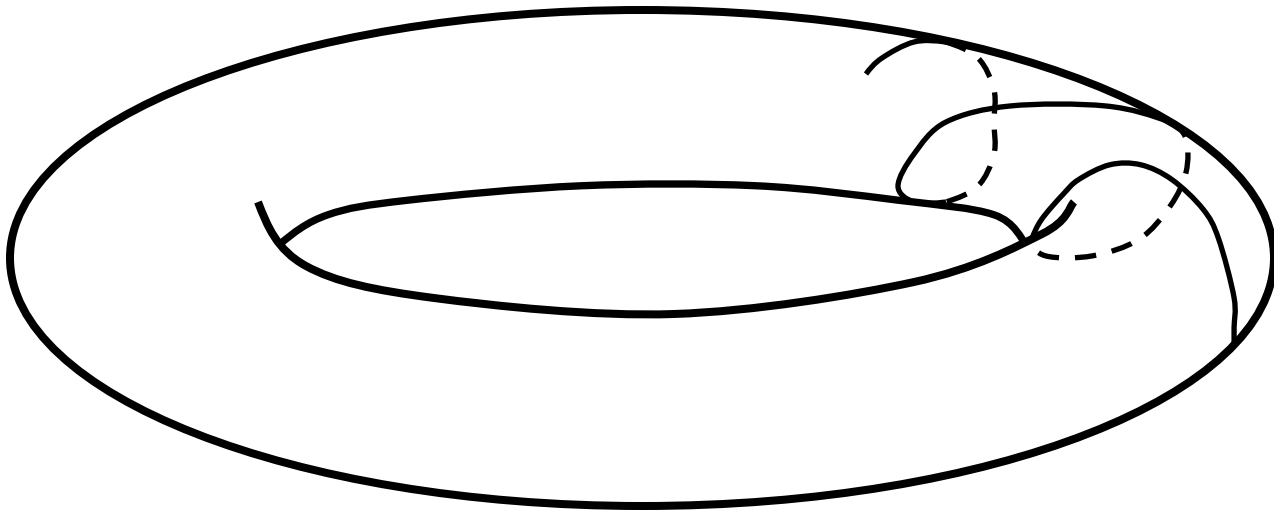


# Behavior of the SALI for **regular motion**

Regular motion occurs on a torus and two different initial deviation vectors **become tangent to the torus, generally having different directions.**

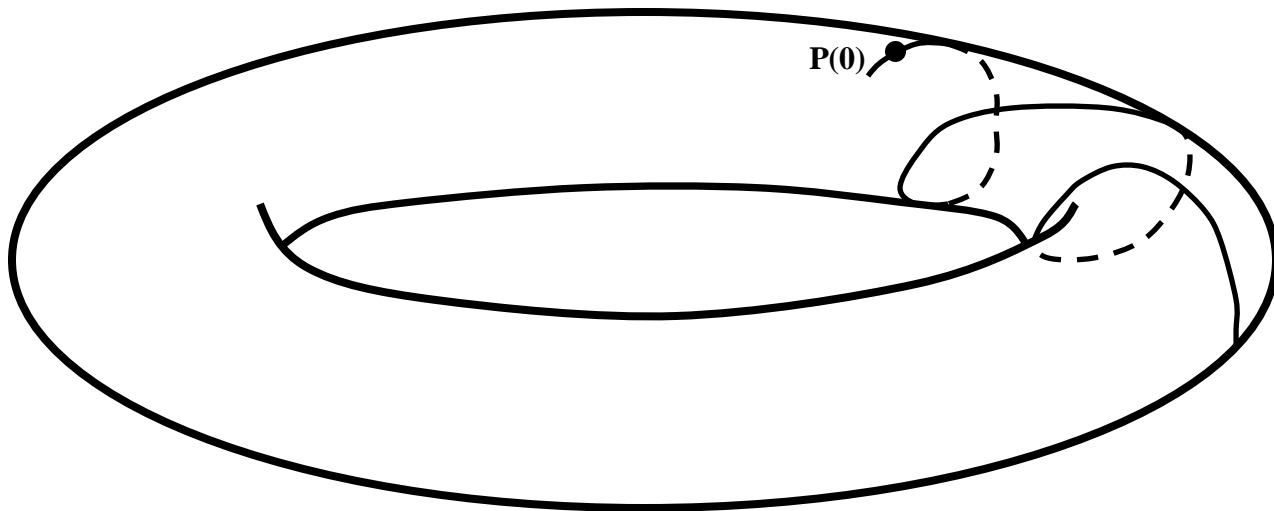
# Behavior of the SALI for **regular motion**

Regular motion occurs on a torus and two different initial deviation vectors **become tangent to the torus, generally having different directions.**



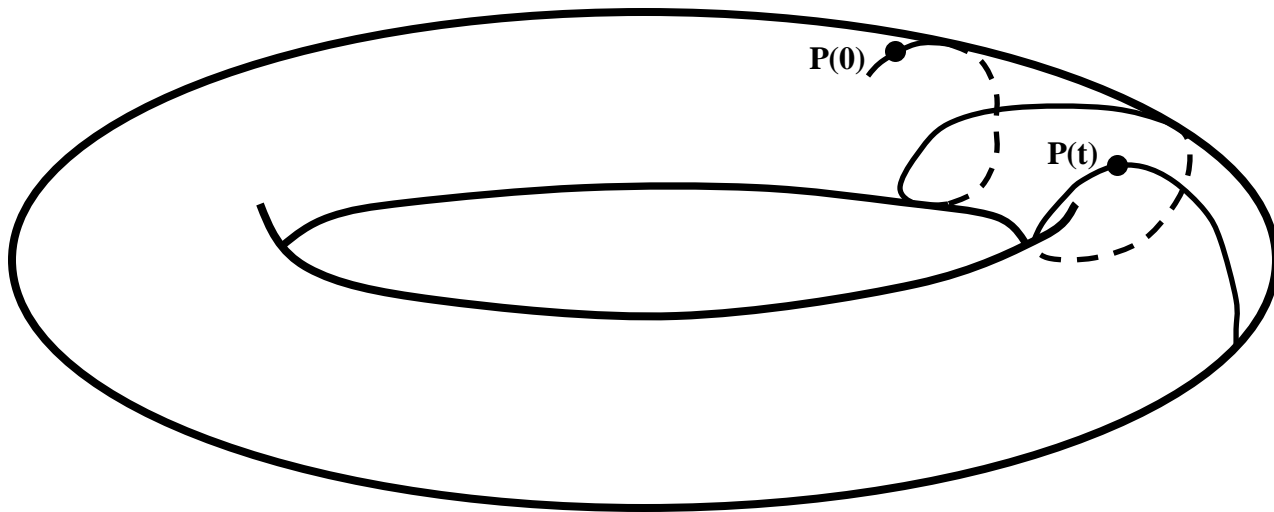
# Behavior of the SALI for **regular motion**

Regular motion occurs on a torus and two different initial deviation vectors **become tangent to the torus, generally having different directions.**



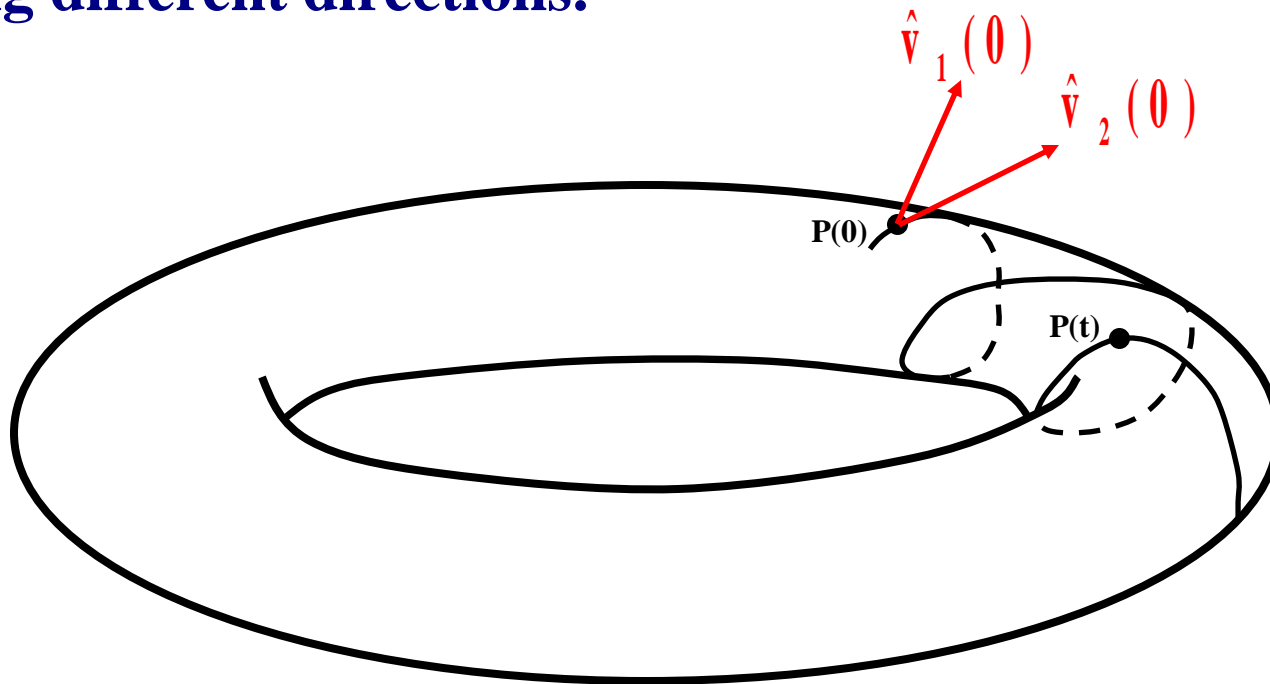
# Behavior of the SALI for **regular motion**

Regular motion occurs on a torus and two different initial deviation vectors **become tangent to the torus, generally having different directions.**



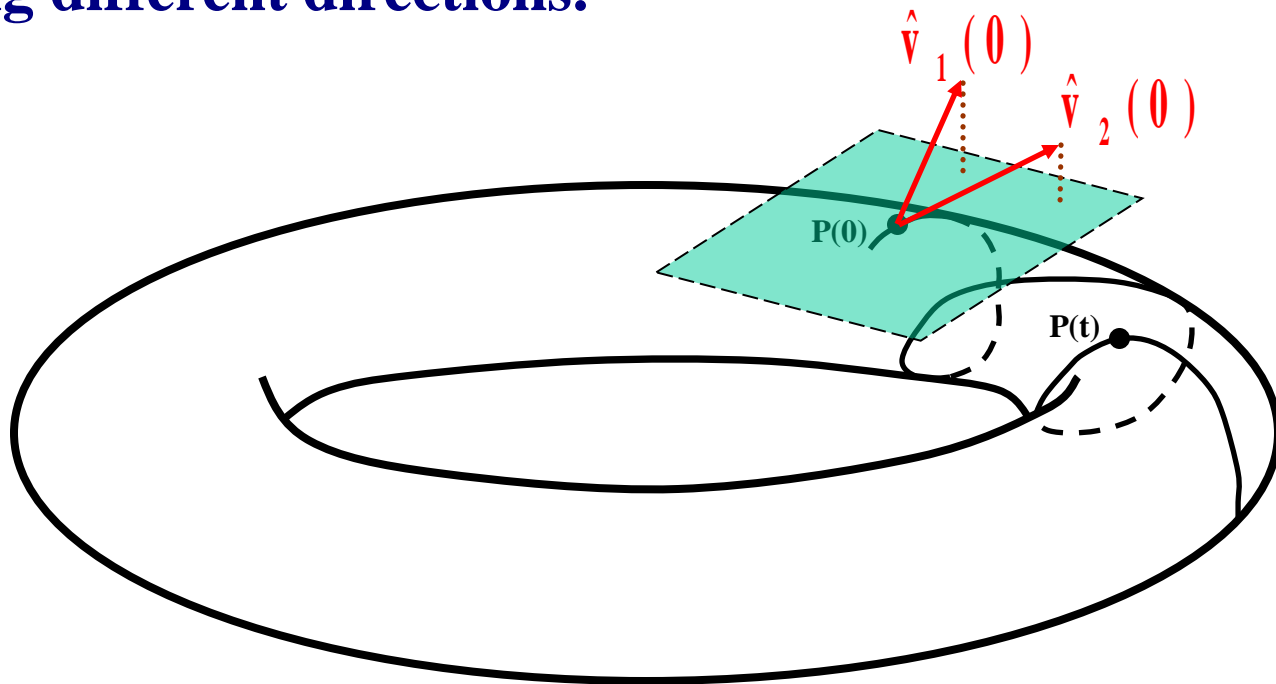
# Behavior of the SALI for **regular motion**

Regular motion occurs on a torus and two different initial deviation vectors **become tangent to the torus**, generally having different directions.



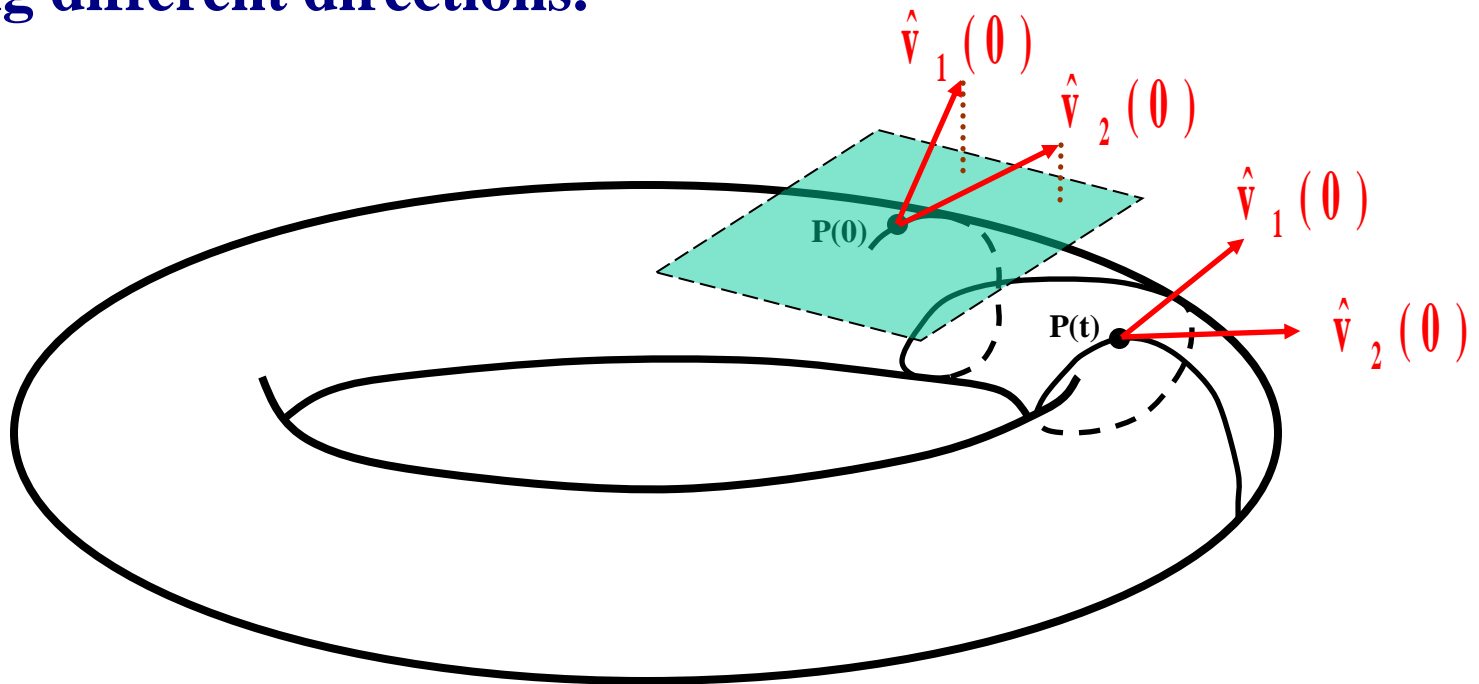
# Behavior of the SALI for **regular motion**

Regular motion occurs on a torus and two different initial deviation vectors **become tangent to the torus**, generally **having different directions**.



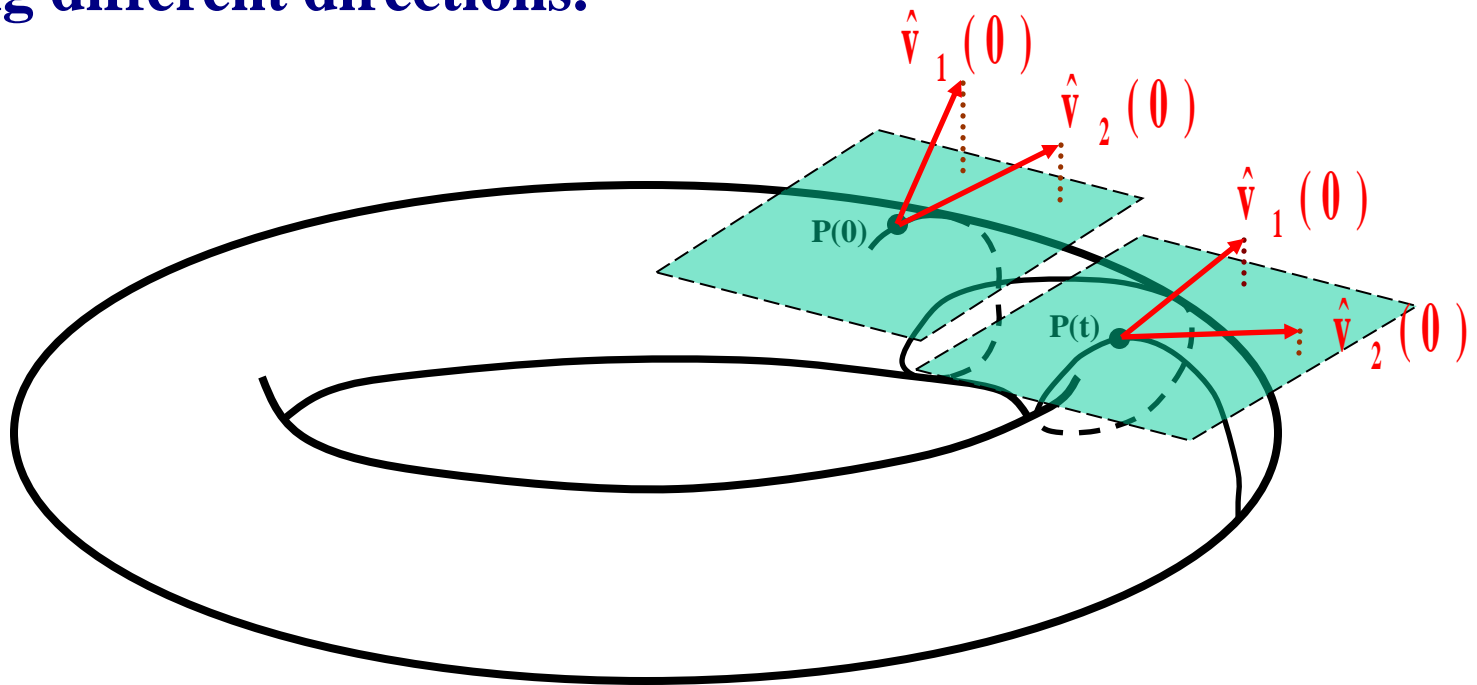
# Behavior of the SALI for **regular motion**

Regular motion occurs on a torus and two different initial deviation vectors **become tangent to the torus**, generally having different directions.



# Behavior of the SALI for **regular motion**

Regular motion occurs on a torus and two different initial deviation vectors **become tangent to the torus**, generally having different directions.





# Applications – Hénon-Heiles system

As an example, we consider the 2D Hénon-Heiles system:

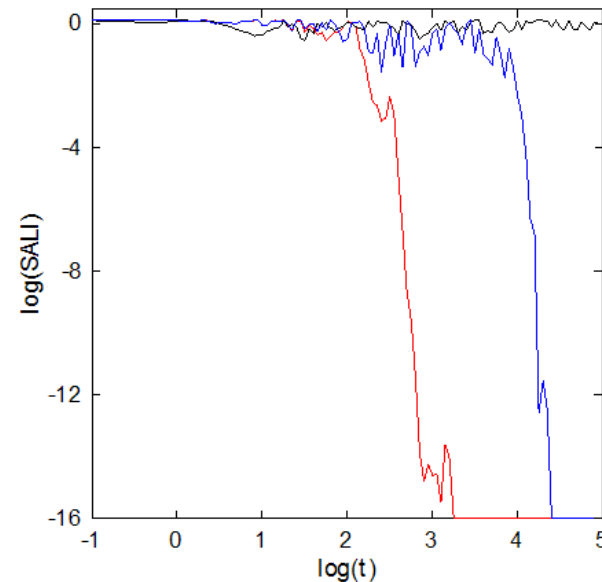
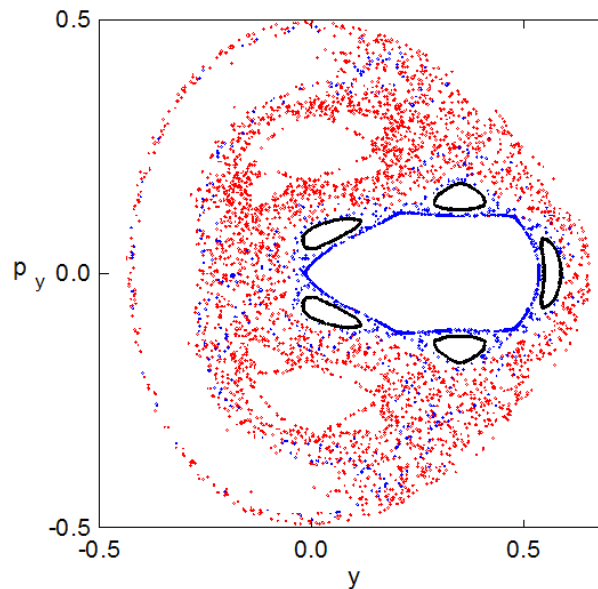
$$H_2 = \frac{1}{2}(p_x^2 + p_y^2) + \frac{1}{2}(x^2 + y^2) + x^2y - \frac{1}{3}y^3$$

For  $E=1/8$  we consider the orbits with initial conditions:

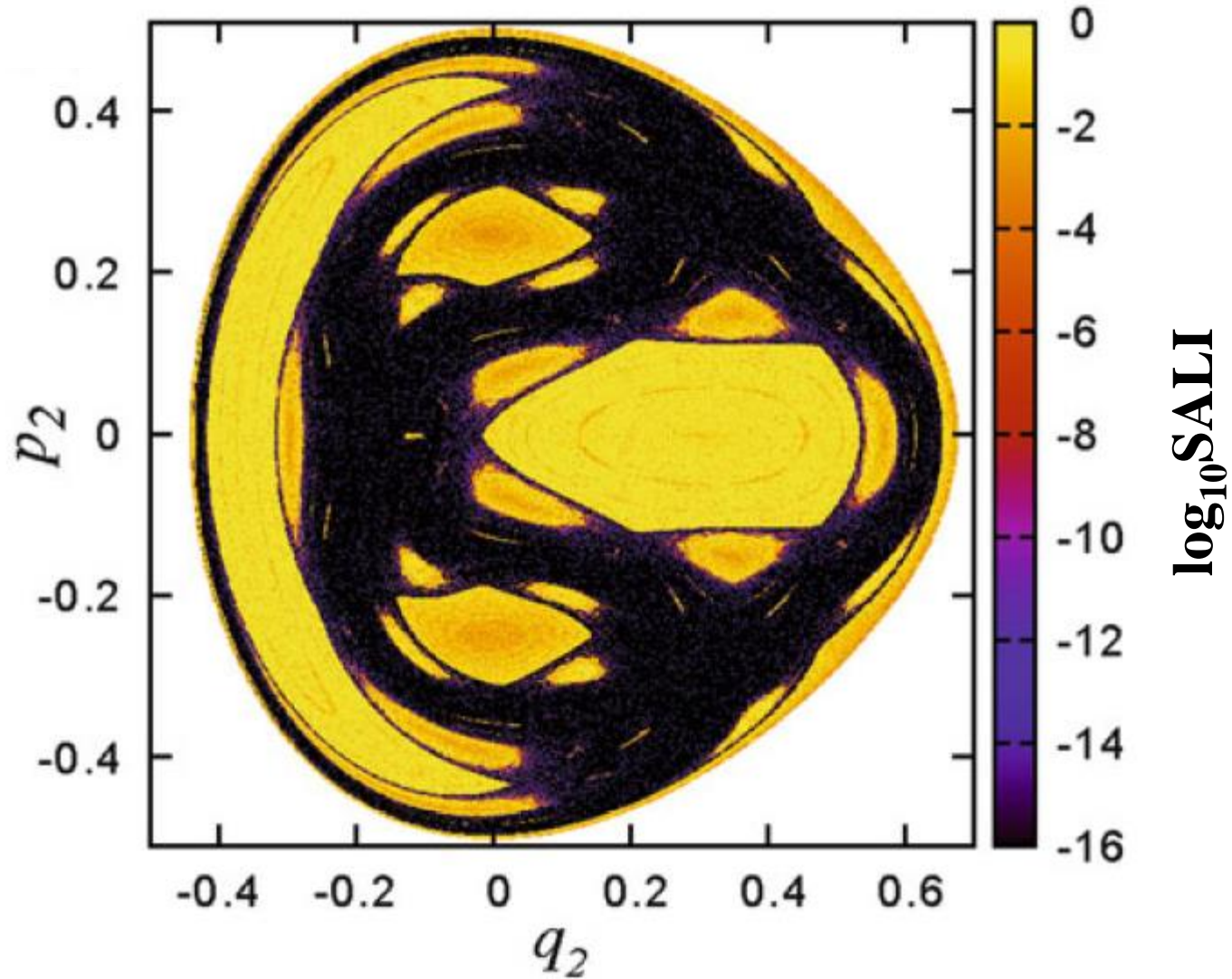
Regular orbit,  $x=0$ ,  $y=0.55$ ,  $p_x=0.2417$ ,  $p_y=0$

Chaotic orbit,  $x=0$ ,  $y=-0.016$ ,  $p_x=0.49974$ ,  $p_y=0$

Chaotic orbit,  $x=0$ ,  $y=-0.01344$ ,  $p_x=0.49982$ ,  $p_y=0$



# Applications – Hénon-Heiles system



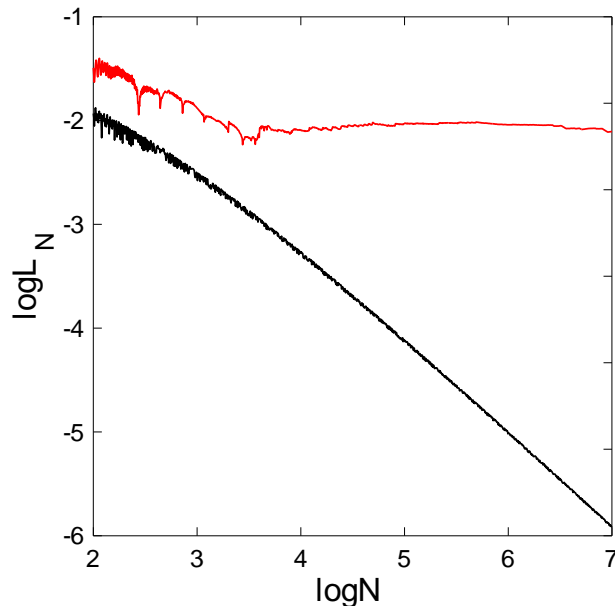
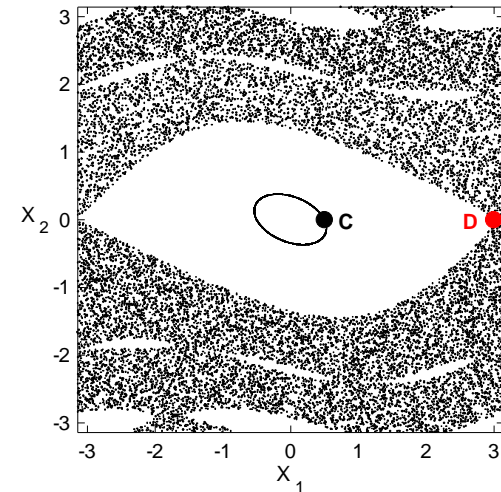
# Applications – 4D map

$$\begin{aligned}
 \mathbf{x}'_1 &= \mathbf{x}_1 + \mathbf{x}_2 \\
 \mathbf{x}'_2 &= \mathbf{x}_2 - \nu \sin(\mathbf{x}_1 + \mathbf{x}_2) - \mu [1 - \cos(\mathbf{x}_1 + \mathbf{x}_2 + \mathbf{x}_3 + \mathbf{x}_4)] \\
 \mathbf{x}'_3 &= \mathbf{x}_3 + \mathbf{x}_4 \\
 \mathbf{x}'_4 &= \mathbf{x}_4 - \kappa \sin(\mathbf{x}_3 + \mathbf{x}_4) - \mu [1 - \cos(\mathbf{x}_1 + \mathbf{x}_2 + \mathbf{x}_3 + \mathbf{x}_4)]
 \end{aligned} \pmod{2\pi}$$

For  $\nu=0.5$ ,  $\kappa=0.1$ ,  $\mu=0.1$  we consider the orbits:

*regular orbit C* with initial conditions  $x_1=0.5$ ,  $x_2=0$ ,  $x_3=0.5$ ,  $x_4=0$ .

*chaotic orbit D* with initial conditions  $x_1=3$ ,  $x_2=0$ ,  $x_3=0.5$ ,  $x_4=0$ .



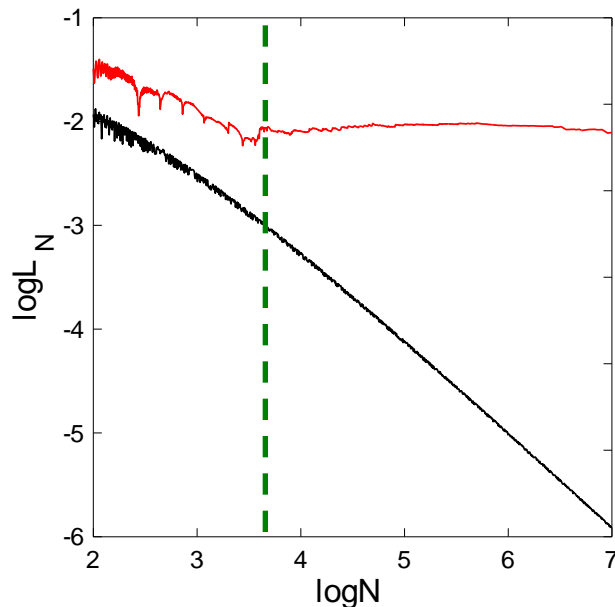
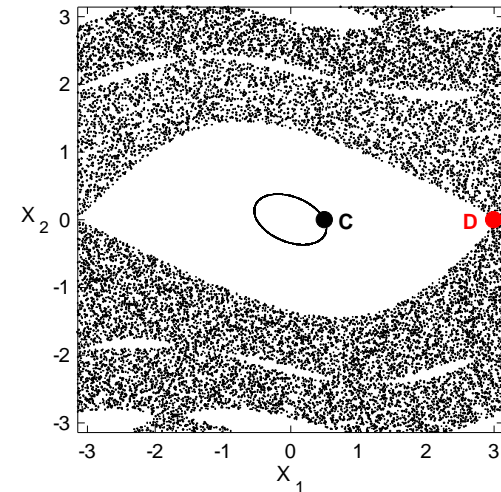
# Applications – 4D map

$$\begin{aligned}
 \mathbf{x}'_1 &= \mathbf{x}_1 + \mathbf{x}_2 \\
 \mathbf{x}'_2 &= \mathbf{x}_2 - \nu \sin(\mathbf{x}_1 + \mathbf{x}_2) - \mu [1 - \cos(\mathbf{x}_1 + \mathbf{x}_2 + \mathbf{x}_3 + \mathbf{x}_4)] \\
 \mathbf{x}'_3 &= \mathbf{x}_3 + \mathbf{x}_4 \\
 \mathbf{x}'_4 &= \mathbf{x}_4 - \kappa \sin(\mathbf{x}_3 + \mathbf{x}_4) - \mu [1 - \cos(\mathbf{x}_1 + \mathbf{x}_2 + \mathbf{x}_3 + \mathbf{x}_4)]
 \end{aligned} \pmod{2\pi}$$

For  $\nu=0.5$ ,  $\kappa=0.1$ ,  $\mu=0.1$  we consider the orbits:

*regular orbit C* with initial conditions  $x_1=0.5$ ,  $x_2=0$ ,  $x_3=0.5$ ,  $x_4=0$ .

*chaotic orbit D* with initial conditions  $x_1=3$ ,  $x_2=0$ ,  $x_3=0.5$ ,  $x_4=0$ .



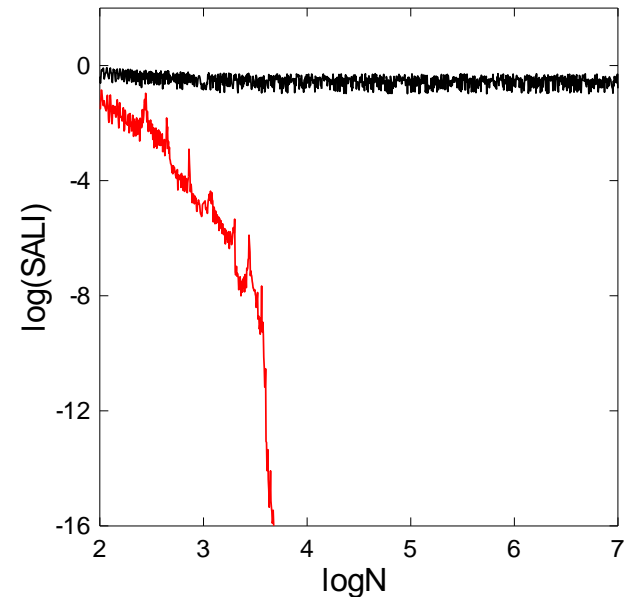
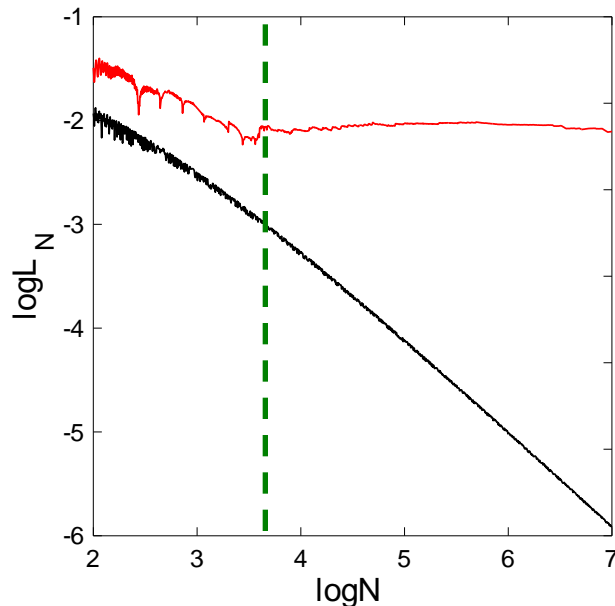
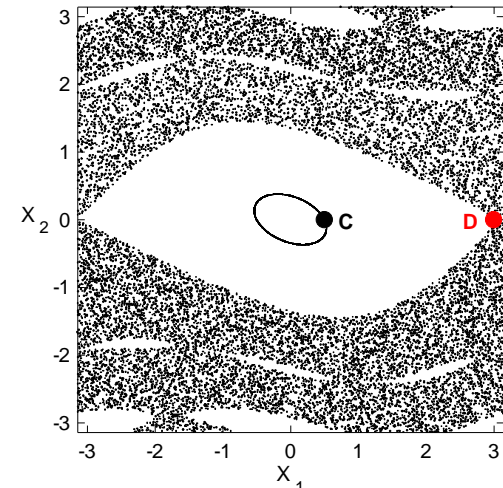
# Applications – 4D map

$$\begin{aligned}
 \mathbf{x}'_1 &= \mathbf{x}_1 + \mathbf{x}_2 \\
 \mathbf{x}'_2 &= \mathbf{x}_2 - \nu \sin(\mathbf{x}_1 + \mathbf{x}_2) - \mu [1 - \cos(\mathbf{x}_1 + \mathbf{x}_2 + \mathbf{x}_3 + \mathbf{x}_4)] \\
 \mathbf{x}'_3 &= \mathbf{x}_3 + \mathbf{x}_4 \\
 \mathbf{x}'_4 &= \mathbf{x}_4 - \kappa \sin(\mathbf{x}_3 + \mathbf{x}_4) - \mu [1 - \cos(\mathbf{x}_1 + \mathbf{x}_2 + \mathbf{x}_3 + \mathbf{x}_4)]
 \end{aligned} \pmod{2\pi}$$

For  $\nu=0.5$ ,  $\kappa=0.1$ ,  $\mu=0.1$  we consider the orbits:

*regular orbit C* with initial conditions  $x_1=0.5$ ,  $x_2=0$ ,  $x_3=0.5$ ,  $x_4=0$ .

*chaotic orbit D* with initial conditions  $x_1=3$ ,  $x_2=0$ ,  $x_3=0.5$ ,  $x_4=0$ .



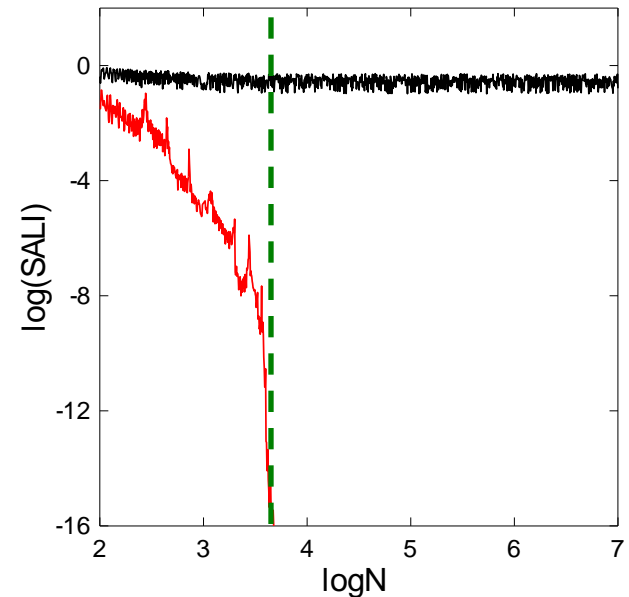
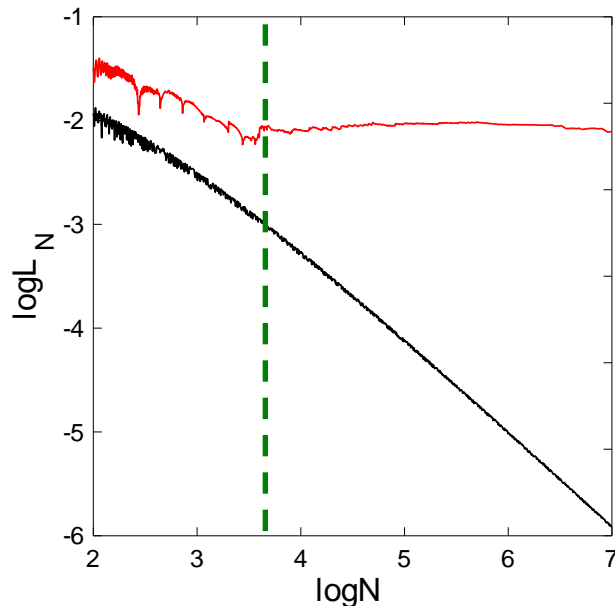
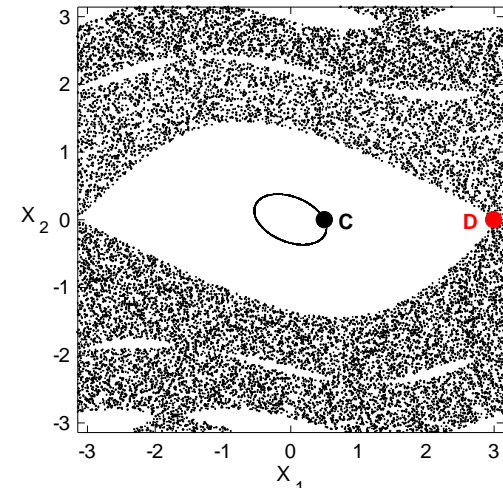
# Applications – 4D map

$$\begin{aligned}
 \mathbf{x}'_1 &= \mathbf{x}_1 + \mathbf{x}_2 \\
 \mathbf{x}'_2 &= \mathbf{x}_2 - \nu \sin(\mathbf{x}_1 + \mathbf{x}_2) - \mu [1 - \cos(\mathbf{x}_1 + \mathbf{x}_2 + \mathbf{x}_3 + \mathbf{x}_4)] \\
 \mathbf{x}'_3 &= \mathbf{x}_3 + \mathbf{x}_4 \\
 \mathbf{x}'_4 &= \mathbf{x}_4 - \kappa \sin(\mathbf{x}_3 + \mathbf{x}_4) - \mu [1 - \cos(\mathbf{x}_1 + \mathbf{x}_2 + \mathbf{x}_3 + \mathbf{x}_4)]
 \end{aligned} \pmod{2\pi}$$

For  $\nu=0.5$ ,  $\kappa=0.1$ ,  $\mu=0.1$  we consider the orbits:

*regular orbit C* with initial conditions  $x_1=0.5$ ,  $x_2=0$ ,  $x_3=0.5$ ,  $x_4=0$ .

*chaotic orbit D* with initial conditions  $x_1=3$ ,  $x_2=0$ ,  $x_3=0.5$ ,  $x_4=0$ .



# **The Generalized ALignment Indices (GALIs) method**

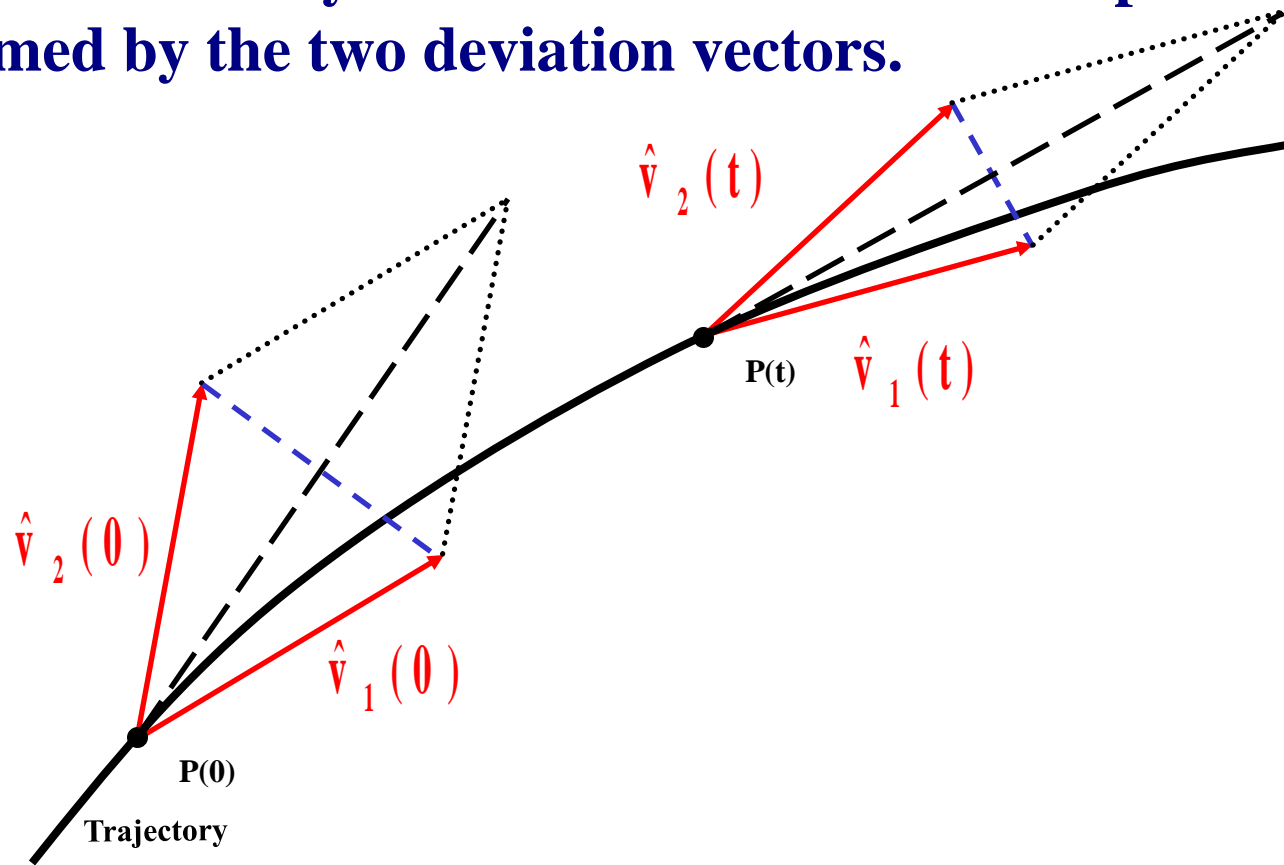
# Definition of the Generalized Alignment Index (GALI)

**SALI effectively measures the 'area' of the parallelogram formed by the two deviation vectors.**



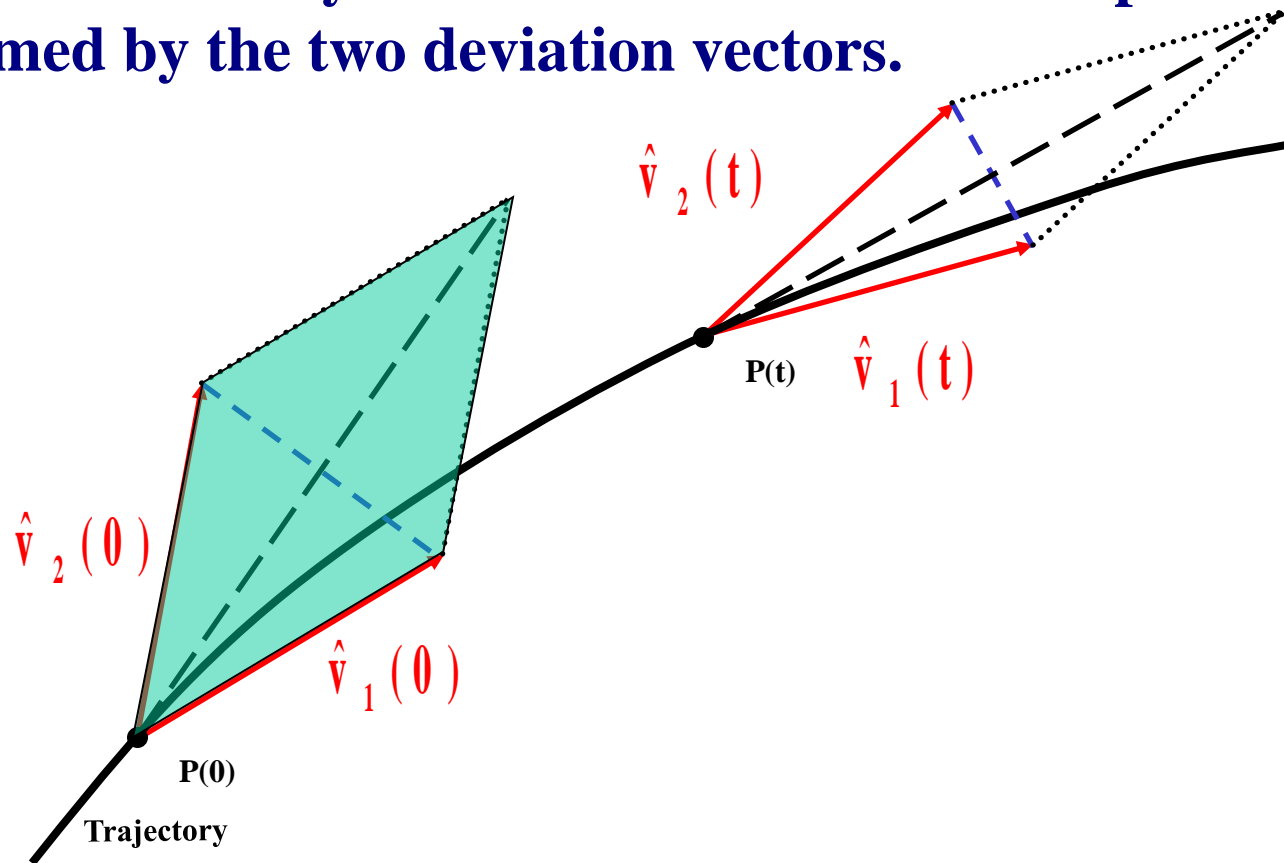
# Definition of the Generalized Alignment Index (GALI)

SALI effectively measures the 'area' of the parallelogram formed by the two deviation vectors.



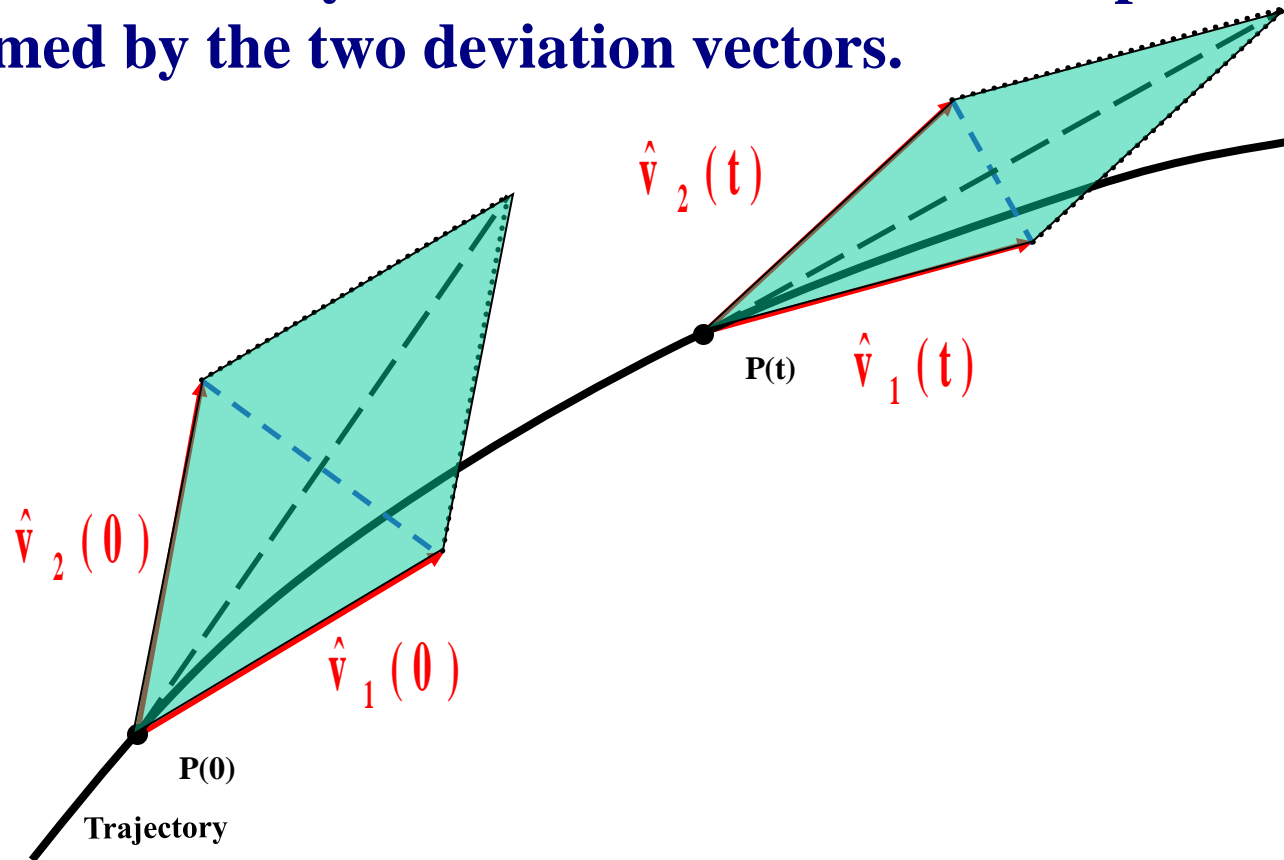
# Definition of the Generalized Alignment Index (GALI)

SALI effectively measures the 'area' of the parallelogram formed by the two deviation vectors.



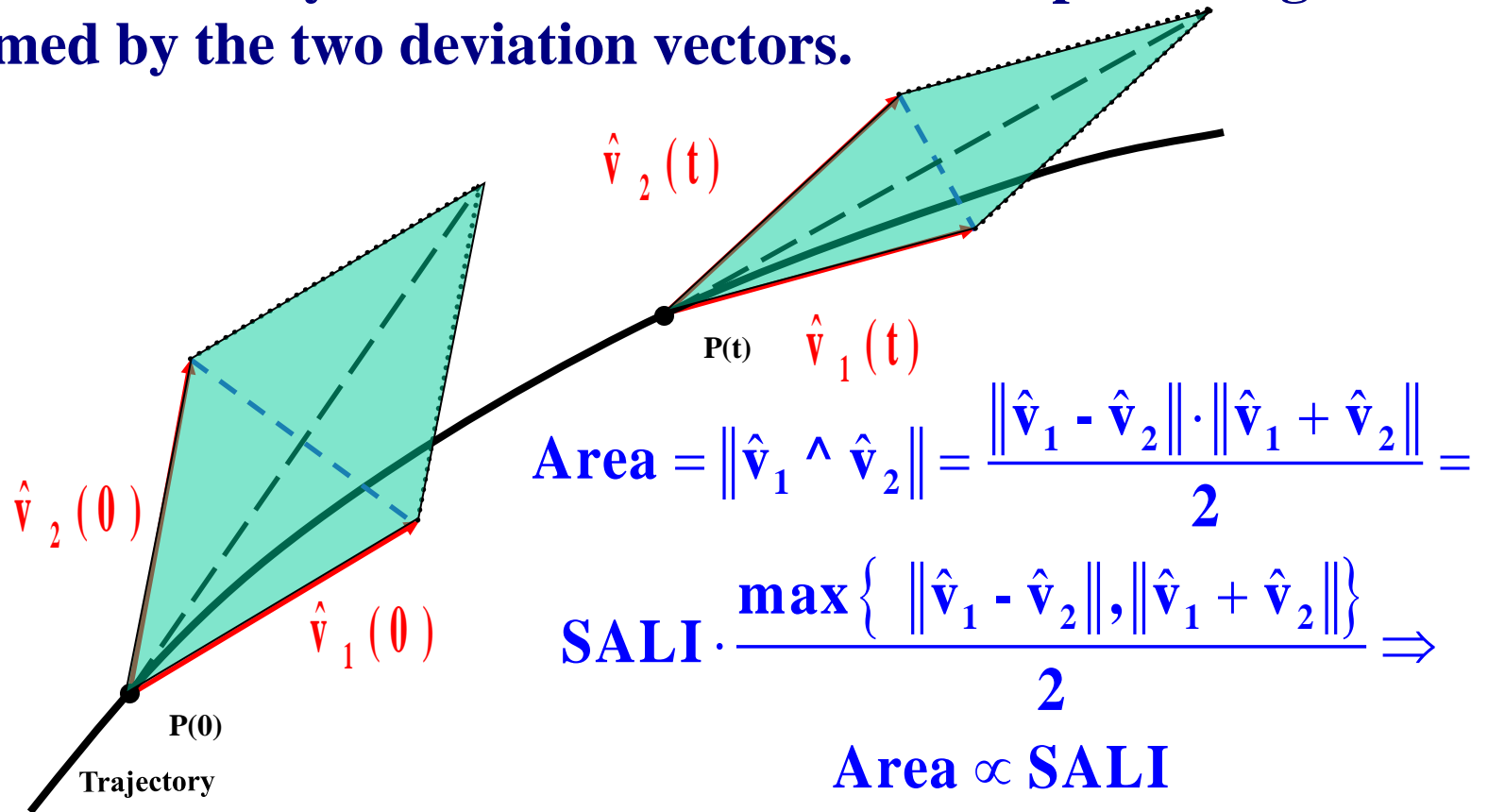
# Definition of the Generalized Alignment Index (GALI)

SALI effectively measures the 'area' of the parallelogram formed by the two deviation vectors.



# Definition of the Generalized Alignment Index (GALI)

SALI effectively measures the ‘area’ of the parallelogram formed by the two deviation vectors.



# Definition of the GALI

In the case of an  $N$  degree of freedom Hamiltonian system or a  $2N$  symplectic map we follow the evolution of

$k$  deviation vectors with  $2 \leq k \leq 2N$ ,

and define (Ch.S., Bountis, Antonopoulos, 2007, Physica D) the Generalized Alignment Index (GALI) of order  $k$  :

$$GALI_k(t) = \left\| \hat{v}_1(t) \wedge \hat{v}_2(t) \wedge \dots \wedge \hat{v}_k(t) \right\|$$

where

$$\hat{v}_1(t) = \frac{v_1(t)}{\|v_1(t)\|}$$

# Behavior of the $GALI_k$ for chaotic motion

$GALI_k$  ( $2 \leq k \leq 2N$ ) tends exponentially to zero with exponents that involve the values of the first  $k$  largest Lyapunov exponents  $\sigma_1, \sigma_2, \dots, \sigma_k$ :

$$G A L I_k(t) \propto e^{-[(\sigma_1 - \sigma_2) + (\sigma_1 - \sigma_3) + \dots + (\sigma_1 - \sigma_k)]t}$$

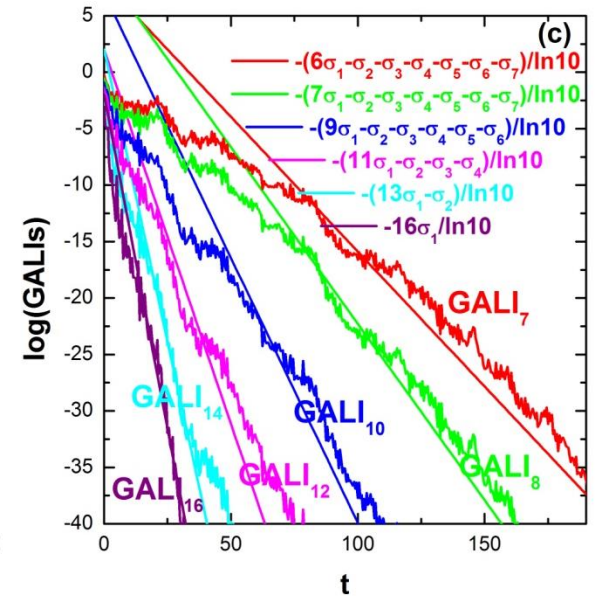
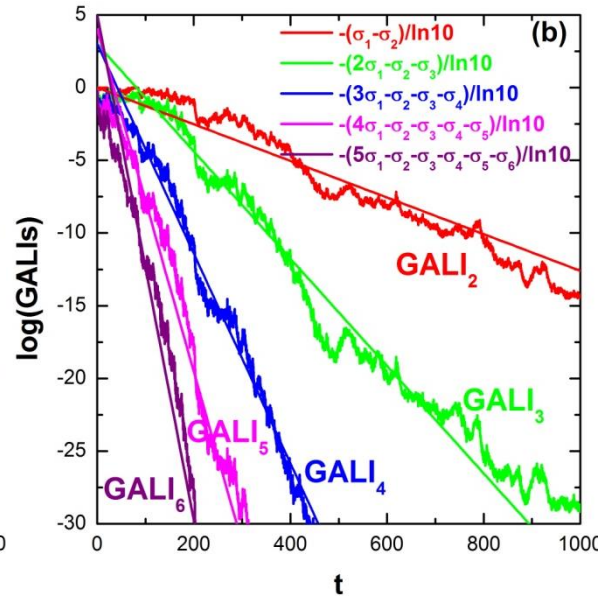
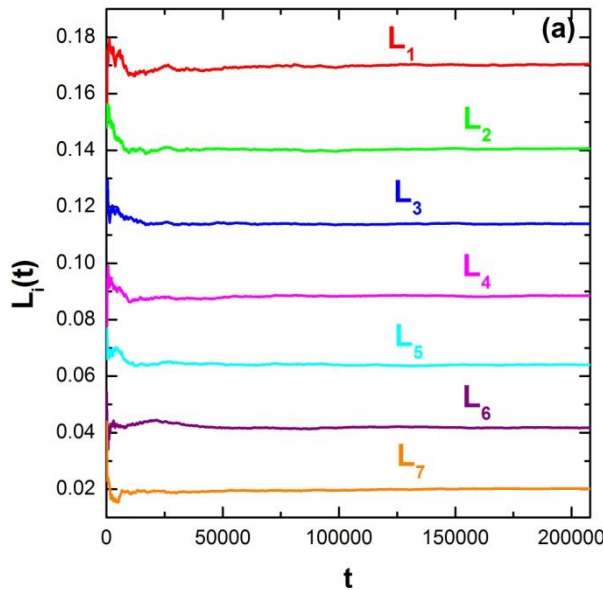
The above relation is valid even if some Lyapunov exponents are equal, or very close to each other.

# Behavior of the $GALI_k$ for chaotic motion

**N particles Fermi-Pasta-Ulam (FPU) system:**

$$H = \frac{1}{2} \sum_{i=1}^N p_i^2 + \sum_{i=0}^N \left[ \frac{1}{2} (q_{i+1} - q_i)^2 + \frac{\beta}{4} (q_{i+1} - q_i)^4 \right]$$

with fixed boundary conditions,  $N=8$  and  $\beta=1.5$ .



# Behavior of the $GALI_k$ for regular motion

If the motion occurs on an **s-dimensional torus** with  $s \leq N$  then the behavior of  $GALI_k$  is given by (Ch.S., Bountis, Antonopoulos, 2008, Eur. Phys. J. Sp. Top.):

$$GALI_k(t) \propto \begin{cases} \text{constant} & \text{if } 2 \leq k \leq s \\ \frac{1}{t^{k-s}} & \text{if } s < k \leq 2N - s \\ \frac{1}{t^{2(k-N)}} & \text{if } 2N - s < k \leq 2N \end{cases}$$

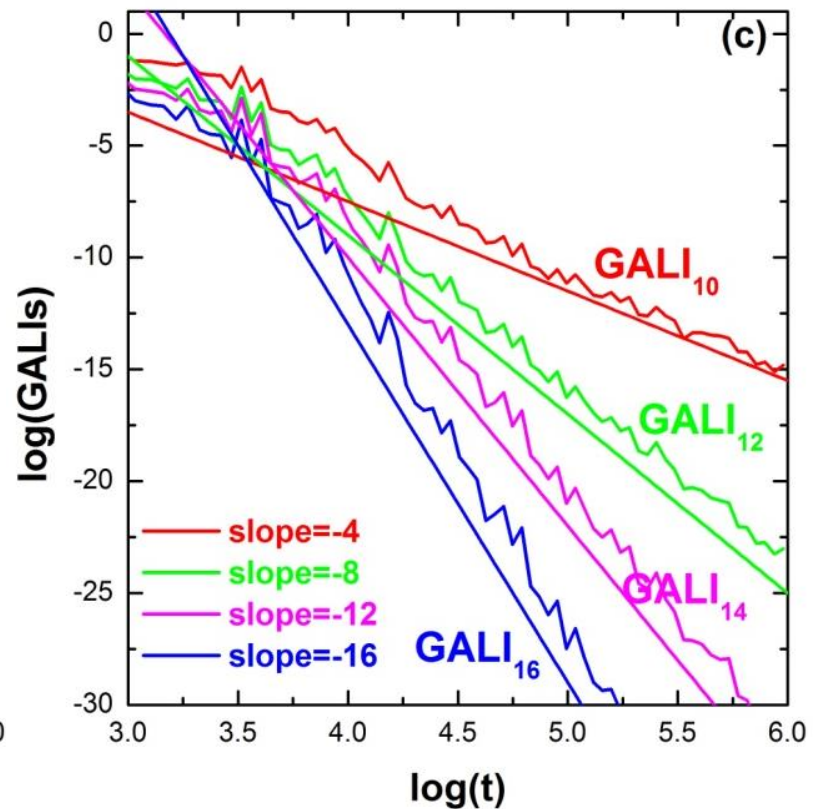
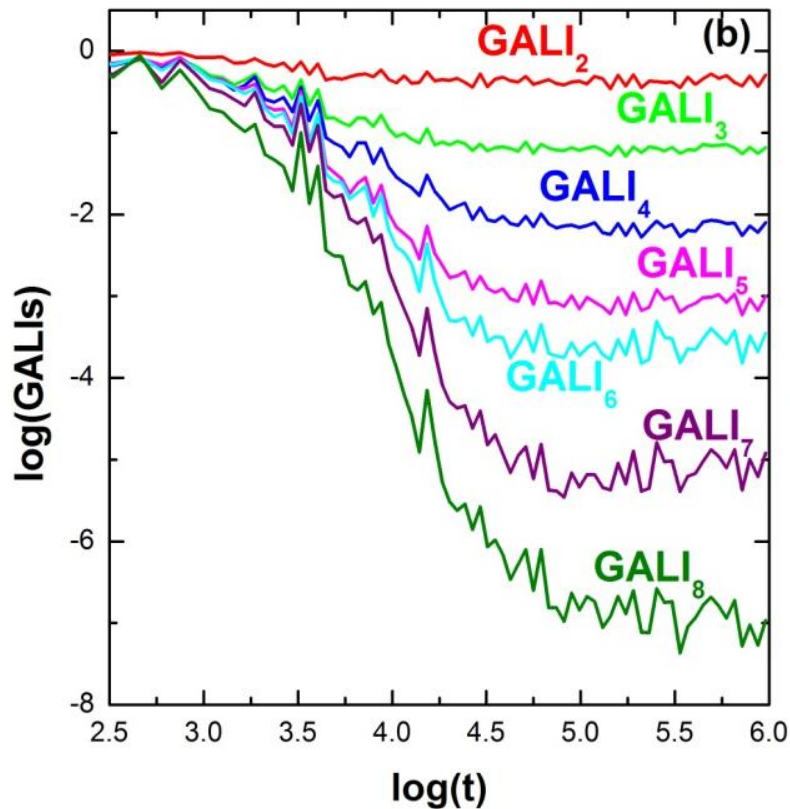
while in the **common case with  $s=N$**  we have :

$$GALI_k(t) \propto \begin{cases} \text{constant} & \text{if } 2 \leq k \leq N \\ \frac{1}{t^{2(k-N)}} & \text{if } N < k \leq 2N \end{cases}$$



# Behavior of the $GALI_k$ for regular motion

**N=8 FPU system**



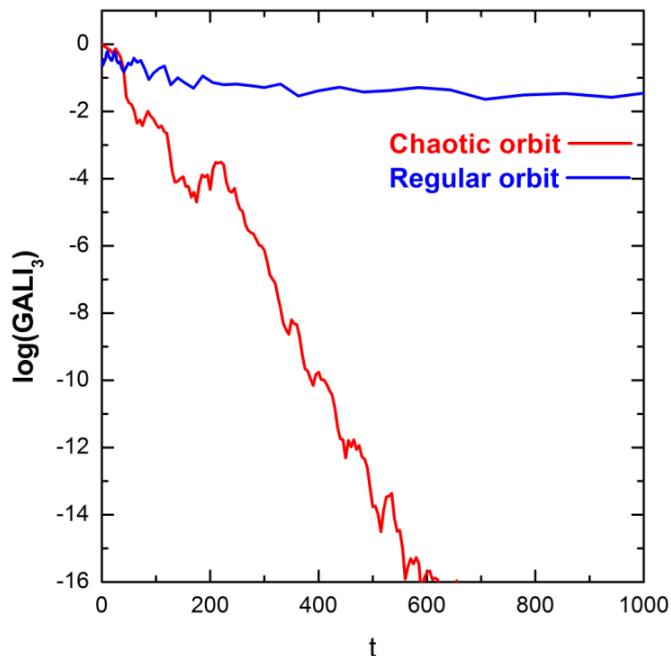
# Global dynamics

- $\text{GALI}_2$  (practically equivalent to the use of SALI)

- $\text{GALI}_N$

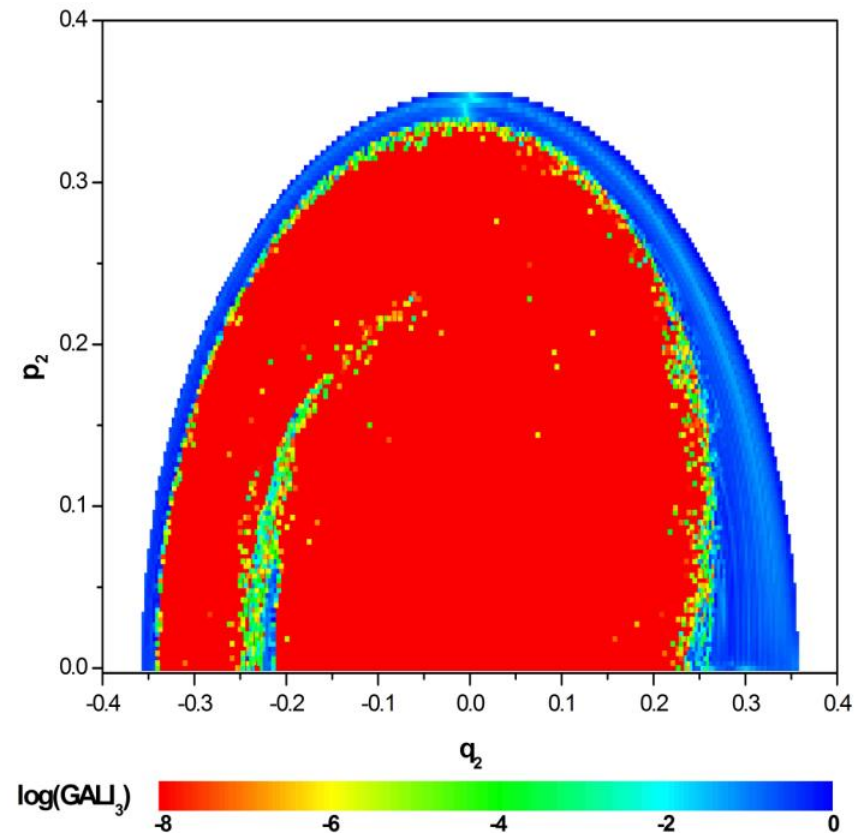
**Chaotic motion:  $\text{GALI}_N \rightarrow 0$   
(exponential decay)**

**Regular motion:  
 $\text{GALI}_N \rightarrow \text{constant} \neq 0$**



## 3D Hamiltonian

Subspace  $q_3=p_3=0$ ,  $p_2 \geq 0$  for  $t=1000$ .



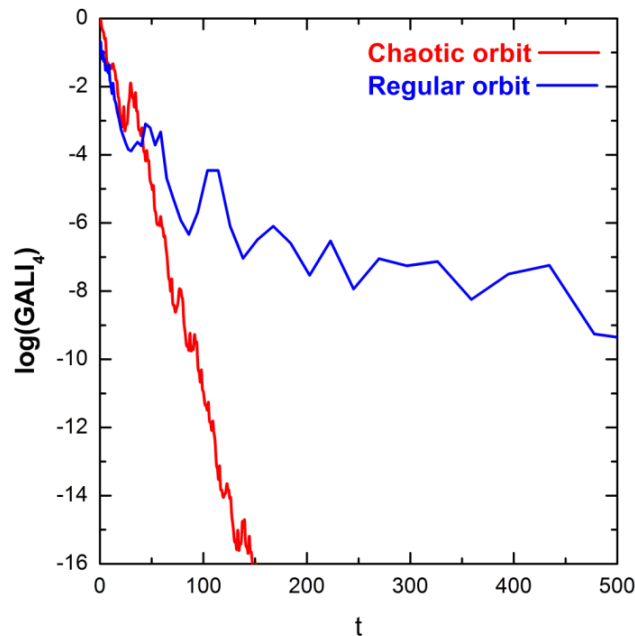
# Global dynamics

$GALI_k$  with  $k > N$

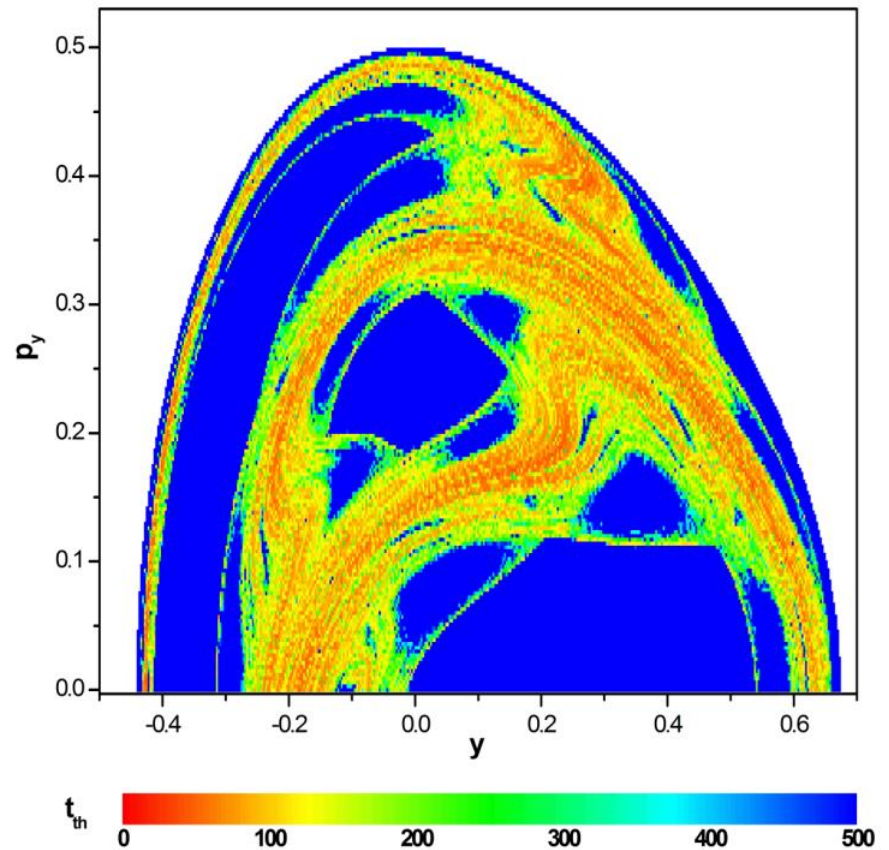
The index tends to zero both for regular and chaotic orbits but with completely different time rates:

**Chaotic motion: exponential decay**

**Regular motion: power law**



2D Hamiltonian (Hénon-Heiles)  
Time needed for  $GALI_4 < 10^{-12}$



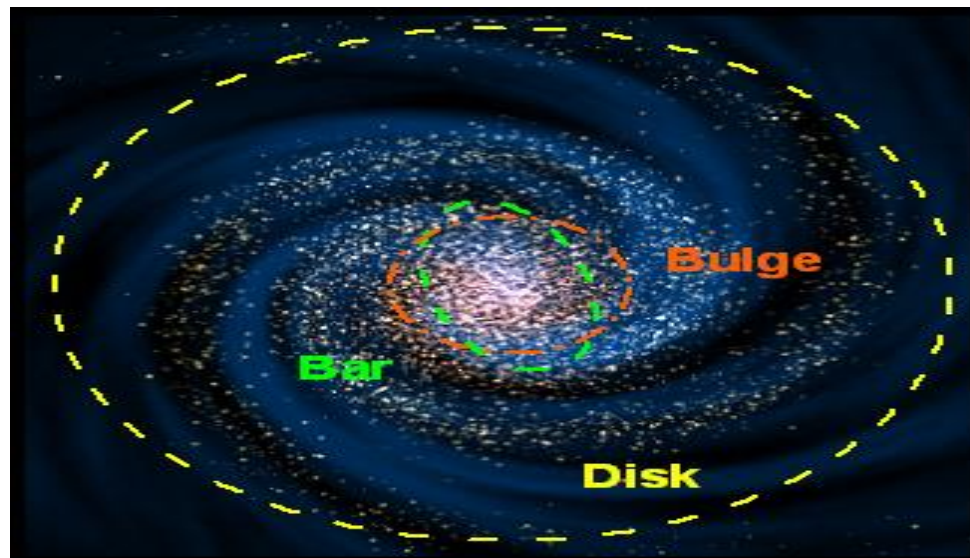
# **A time-dependent Hamiltonian system**

# Barred galaxies

NGC 1433



NGC 2217



# Barred galaxy model

The 3D bar rotates around its short  $z$ -axis ( $x$ : long axis and  $y$ : intermediate). The Hamiltonian that describes the motion for this model is:

$$H = \frac{1}{2}(p_x^2 + p_y^2 + p_z^2) + V(x, y, z) - \Omega_b(xp_y - yp_x) \equiv \text{Energy}$$

This model consists of the superposition of potentials describing an **axisymmetric** part and a **bar** component of the galaxy (**Manos, Bountis, Ch.S., 2013, J. Phys. A**).

**a) Axisymmetric component:**

i) **Plummer sphere:**

$$V_{\text{sphere}}(x, y, z) = -\frac{GM_s}{\sqrt{x^2 + y^2 + z^2 + \epsilon_s^2}}$$

ii) **Miyamoto–Nagai disc:**

$$V_{\text{disc}}(x, y, z) = -\frac{GM_D}{\sqrt{x^2 + y^2 + (A + \sqrt{B^2 + z^2})^2}}$$

**b) Bar component:**  $V_{\text{bar}}(x, y, z) = -\pi Gabc \frac{\rho_c}{n+1} \int_{\lambda}^{\infty} \frac{du}{\Delta(u)} (1 - m^2(u))^{n+1},$

**(Ferrers bar)**

$$\rho_c = \frac{105}{32\pi} \frac{GM_B}{abc}$$

$$\text{where } m^2(u) = \frac{x^2}{a^2 + u} + \frac{y^2}{b^2 + u} + \frac{z^2}{c^2 + u}, \Delta^2(u) = (a^2 + u)(b^2 + u)(c^2 + u),$$

$n$ : positive integer ( $n = 2$  for our model),  $\lambda$ : the unique positive solution of  $m^2(\lambda) = 1$

**Its density is:**

$$\rho = \begin{cases} \rho_c (1 - m^2)^n, & \text{for } m \leq 1 \\ 0, & \text{for } m > 1 \end{cases}, \text{ where } m^2 = \frac{x^2}{a^2} + \frac{y^2}{b^2} + \frac{z^2}{c^2}, a > b > c \text{ and } n = 2.$$



# Time-dependent barred galaxy model

The 3D bar rotates around its short  $z$ -axis ( $x$ : long axis and  $y$ : intermediate). The Hamiltonian that describes the motion for this model is:

$$H = \frac{1}{2}(p_x^2 + p_y^2 + p_z^2) + V(x, y, z, t) - \Omega_b(xp_y - yp_x) \equiv \text{Energy}$$

This model consists of the superposition of potentials describing an **axisymmetric** part and a **bar** component of the galaxy (Manos, Bountis, Ch.S., 2013, J. Phys. A).

**a) Axisymmetric component:**

$$M_S + M_B(t) + M_D(t) = 1, \text{ with } M_B(t) = M_B(0) + \alpha t$$

i) **Plummer sphere:**

$$V_{\text{sphere}}(x, y, z) = -\frac{GM_S}{\sqrt{x^2 + y^2 + z^2 + \epsilon_s^2}}$$

ii) **Miyamoto–Nagai disc:**

$$V_{\text{disc}}(x, y, z) = -\frac{GM_D(t)}{\sqrt{x^2 + y^2 + (A + \sqrt{B^2 + z^2})^2}}$$

**b) Bar component:**  $V_{\text{bar}}(x, y, z) = -\pi Gabc \frac{\rho_c}{n+1} \int_{\lambda}^{\infty} \frac{du}{\Delta(u)} (1 - m^2(u))^{n+1},$

(Ferrers bar)

$$\rho_c = \frac{105}{32\pi} \frac{GM_B(t)}{abc}$$

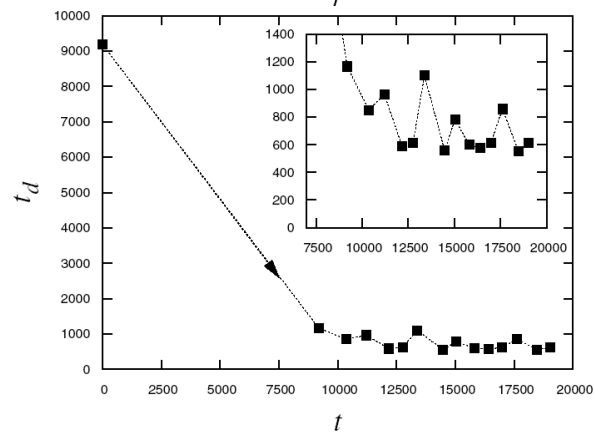
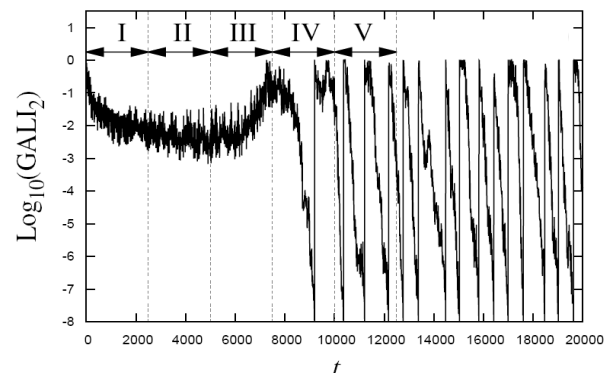
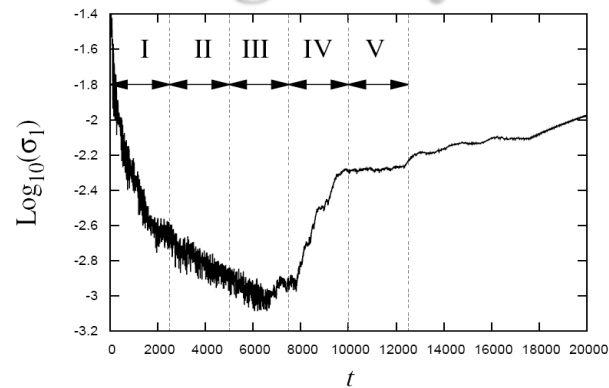
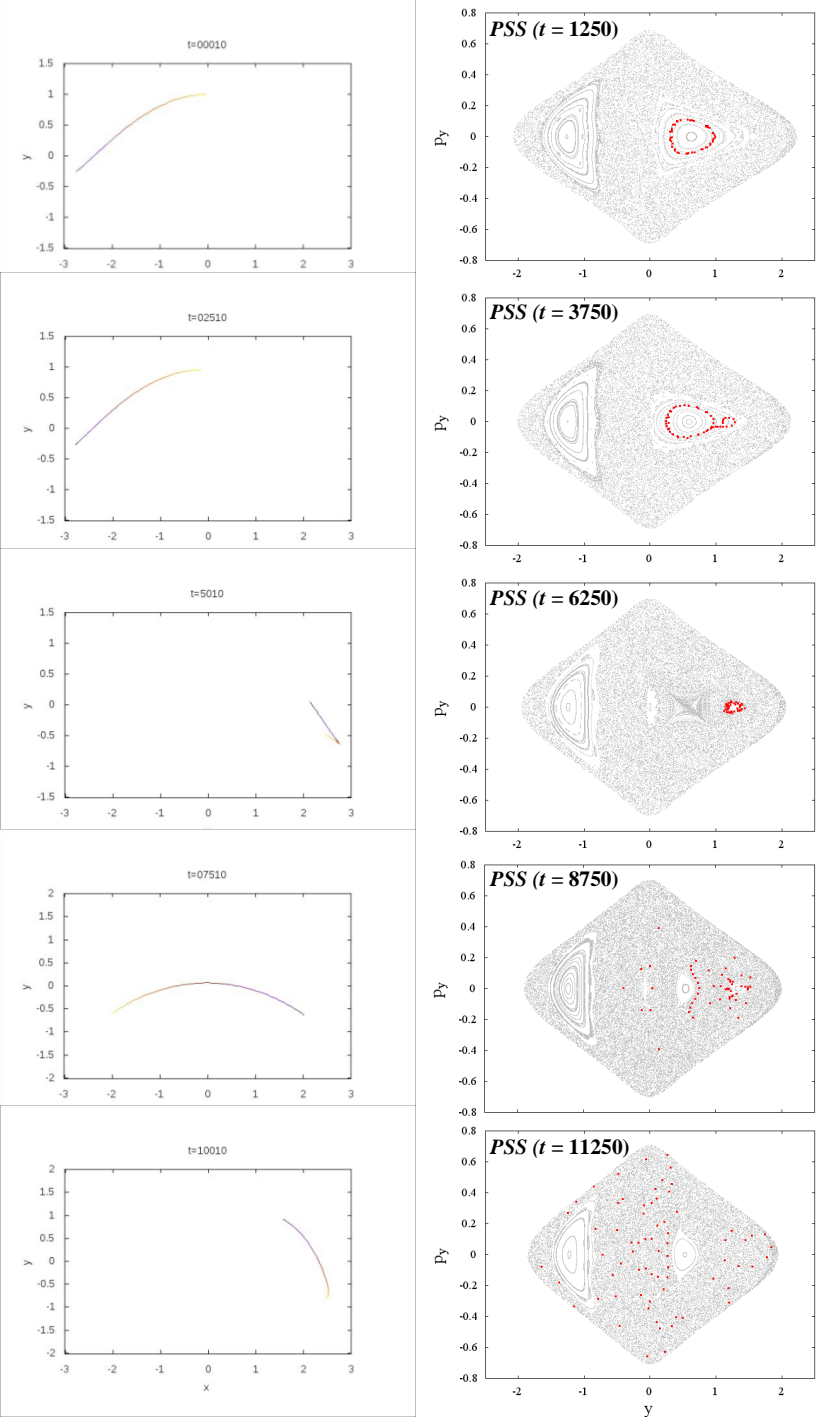
$$\text{where } m^2(u) = \frac{x^2}{a^2 + u} + \frac{y^2}{b^2 + u} + \frac{z^2}{c^2 + u}, \Delta^2(u) = (a^2 + u)(b^2 + u)(c^2 + u),$$

$n$ : positive integer ( $n = 2$  for our model),  $\lambda$ : the unique positive solution of  $m^2(\lambda) = 1$

Its density is:

$$\rho = \begin{cases} \rho_c (1 - m^2)^n, & \text{for } m \leq 1 \\ 0, & \text{for } m > 1 \end{cases}, \text{ where } m^2 = \frac{x^2}{a^2} + \frac{y^2}{b^2} + \frac{z^2}{c^2}, a > b > c \text{ and } n = 2.$$

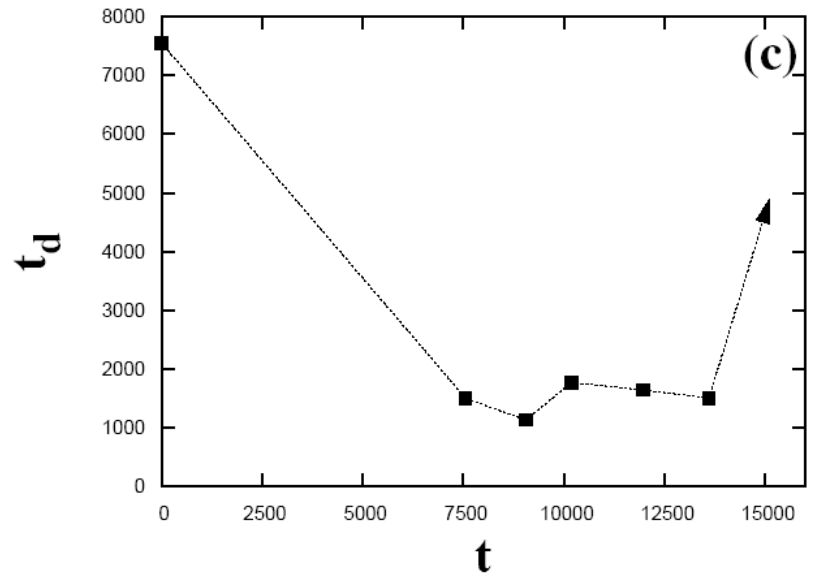
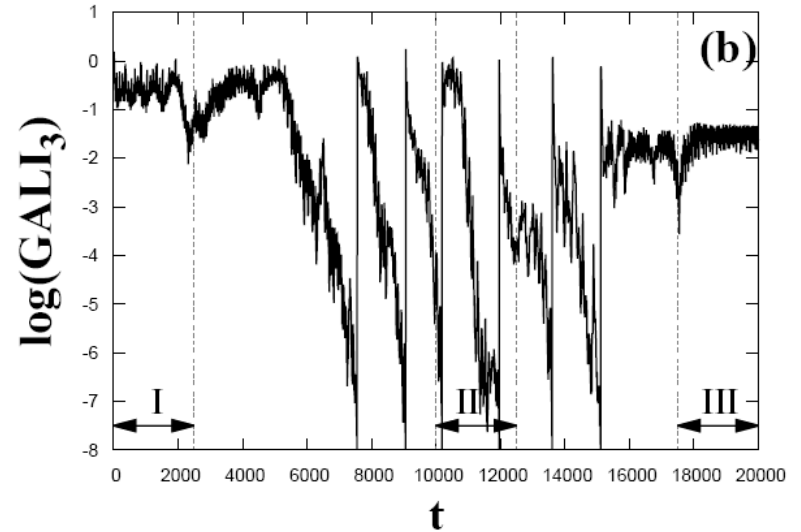
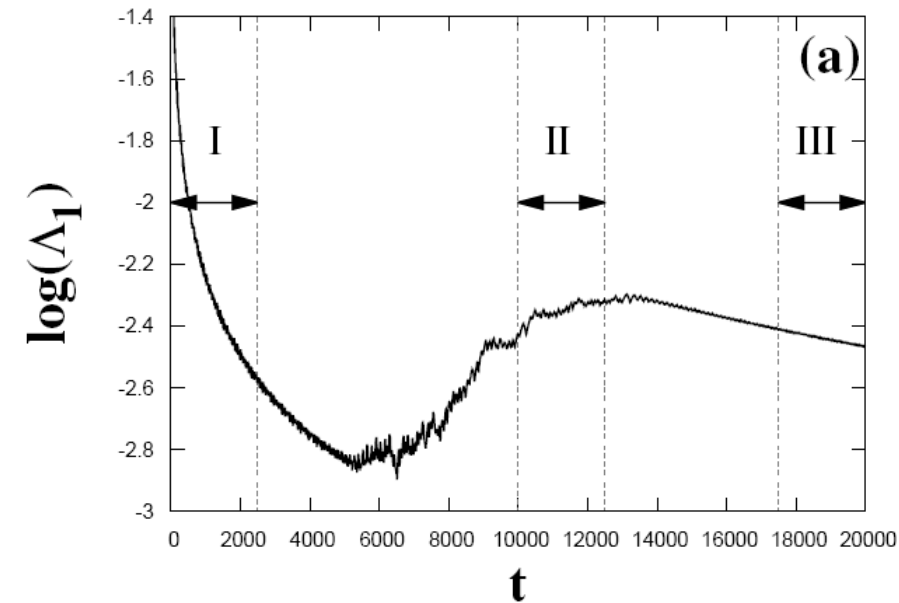
# Time-dependent 2D barred galaxy model





# Time-dependent 3D barred galaxy model

Interplay between chaotic and regular motion



# Summary

- The Smaller (SALI) and the Generalized (GALI) ALignment Index methods are **fast, efficient and easy to compute chaos indicator**.
- Behaviour of the Generalized ALignment Index of order  $k$  ( $GALI_k$ ):
  - ✓ **Chaotic motion: it tends exponentially to zero**
  - ✓ **Regular motion: it fluctuates around non-zero values (or goes to zero following power-laws)**
- $GALI_k$  indices :
  - ✓ **can distinguish rapidly and with certainty between regular and chaotic motion**
  - ✓ **can be used to characterize individual orbits as well as "chart" chaotic and regular domains in phase space**
  - ✓ **can identify regular motion on low-dimensional tori**
  - ✓ **are perfectly suited for studying the global dynamics of multidimensional systems, as well as of time-dependent models**

# Main References

- **Lyapunov exponents**
  - ✓ Ch.S. (2010) Lect. Notes Phys., 790, 63
- **Reviews on SALI and GALI**
  - ✓ Bountis T C & Ch.S. (2012) ‘Complex Hamiltonian Dynamics’, Chapter 5, Springer Series in Synergetics
  - ✓ Ch.S. & Manos T (2016) Lect. Notes Phys., 915, 129
- **SALI**
  - ✓ Ch.S. (2001) J. Phys. A, 34, 10029
  - ✓ Ch.S., Antonopoulos Ch, Bountis T C & Vrahatis M N (2003) Prog. Theor. Phys. Supp., 150, 439
  - ✓ Ch.S., Antonopoulos Ch, Bountis T C & Vrahatis M N (2004) J. Phys. A, 37, 6269
  - ✓ Bountis T & Ch.S. (2006) Nucl. Inst Meth. Phys Res. A, 561, 173
  - ✓ Boreaux J, Carletti T, Ch.S. & Vittot M (2012) Com. Nonlin. Sci. Num. Sim., 17, 1725
  - ✓ Boreaux J, Carletti T, Ch.S., Papaphilippou Y & Vittot M (2012) Int. J. Bif. Chaos, 22, 1250219
- **GALI**
  - ✓ Ch.S., Bountis T C & Antonopoulos Ch (2007) Physica D, 231, 30
  - ✓ Ch.S., Bountis T C & Antonopoulos Ch (2008) Eur. Phys. J. Sp. Top., 165, 5
  - ✓ Gerlach E, Eggl S & Ch.S. (2012) Int. J. Bif. Chaos, 22, 1250216
  - ✓ Manos T, Ch.S. & Antonopoulos Ch (2012) Int. J. Bif. Chaos, 22, 1250218
  - ✓ Manos T, Bountis T & Ch.S. (2013) J. Phys. A, 46, 254017
  - ✓ Moges H, Manos T & Ch.S. (2020) Nonlin. Phenom. Complex Syst., in press, nlin.CD/2001.00803

# A ...shameless promotion

## Contents

Lecture Notes in Physics 915

Charalampos (Haris) Skokos  
Georg A. Gottwald  
Jacques Laskar *Editors*

# Chaos Detection and Predictability

 Springer

1. **Parlitz:** Estimating Lyapunov Exponents from Time Series
2. **Lega, Guzzo, Froeschlé:** Theory and Applications of the Fast Lyapunov Indicator (FLI) Method
3. **Barrio:** Theory and Applications of the Orthogonal Fast Lyapunov Indicator (OFLI and OFLI2) Methods
4. **Cincotta, Giordano:** Theory and Applications of the Mean Exponential Growth Factor of Nearby Orbits (MEGNO) Method
5. **Ch.S., Manos:** The Smaller (SALI) and the Generalized (GALI) Alignment Indices: Efficient Methods of Chaos Detection
6. **Sándor, Maffione:** The Relative Lyapunov Indicators: Theory and Application to Dynamical Astronomy
7. **Gottwald, Melbourne:** The 0-1 Test for Chaos: A Review
8. **Siebert, Kantz:** Prediction of Complex Dynamics: Who Cares About Chaos?